DYNAMICS OF FEW-CLUSTER SYSTEMS

by

Mantile Leslie Lekala

Submitted in accordance with the requirements for the degree of

Doctor of Philosophy

in the subject

Physics

at the

University of South Africa

Promoter : Professor S.A. Sofianos

Joint promoter : Professor M. Braun

2004

ACKNOWLEDGEMENTS

It is a great honour and privilege to thank the following people:

- Professor S. A. Sofianos, my promoter, who has ungrudgingly offered his assistance, guidance, mentoring, and full support throughout. I thank him for his patience, due diligence, and more importantly to have introduced me in the first place to the exciting field of Few-Body Physics.
- Professor M. Braun, my co-promoter, for continuous support. His guidance on numerical aspects at the early stages of this thesis is highly appreciated.
- Dr V. Roudnev of St. Petersburg University, Russia, who introduced me to the formalism of total-angular-momentum decomposition of the Faddeev equations, and the related numerics.
- A great indebtedness of gratitude goes to my family: Lineo and Mathapelo, for all their unwavering support and encouragement. I thank also all members of my family and in-laws for moral support.

You have all, in respective different ways, helped make this thesis a reality.

Student Number : **454-288-6**

"I declare that **Dynamics of Few-Cluster Systems** is my own work and that all the sources that I have used or quoted have been indicated and acknowledged by means of complete references".

_____ _____

Mantile Leslie Lekala Pretoria, 2004

SUMMARY

The three-body bound state problem is considered using configuration-space Faddeev equations within the framework of the total-angular-momentum representation. Different three-body systems are considered, the main concern of the investigation being the *i*) calculation of binding energies for weakly bounded trimers, *ii*) handling of systems with a plethora of states, *iii*) importance of three-body forces in trimers, and *iv*) the development of a numerical technique for reliably handling three-dimensional integrodifferential equations. In this respect we considered the three-body nuclear problem, the ^{4}He trimer, and the Ozone ($^{16}O_3$) system.

In practice, we solve the three-dimensional equations using the orthogonal collocation method with triquintic Hermite splines. The resulting eigenvalue equation is handled using the explicitly Restarted Arnoldi Method in conjunction with the Chebyshev polynomials to improve convergence. To further facilitate convergence, the grid knots are distributed quadratically, such that there are more grid points in regions where the potential is stronger. The so-called tensor-trick technique is also employed to handle the large matrices involved. The computation of the many and dense states for the Ozone case is best implemented using the global minimization program PANMIN based on the well known MERLIN optimization program.

Stable results comparable to those of other methods were obtained for both nucleonic and molecular systems considered.

Key Words: Three-Body Bound State; Configuration Space Faddeev Equations; Total-Angular-Momentum Representation; Three-Body Forces; Orthogonal Spline Collocation; Weakly Bounded Trimers.

Contents

"Reading maketh a full man. Conference a ready man. And writing an exact man."

Francis Bacon (1561 - 1626)

Chapter 1

Introduction

The study of dynamics of non-relativistic quantum mechanical systems consisting of few particles, received a considerable attention and has been an active field of research for several decades. As early as 1936 Bethe discussed in detail the role of three-particle systems in describing the static properties of the nuclear matter [1]. In the fifties the emphasis was shifted to the few-nucleon systems where a large number of theoretical and experimental investigations on three and four nucleon reactions were made. This shift can be attributed to the increase in interest on the three-nucleon and four-nucleon fusion and disintegration reactions. The methodology and approach of these works can be seen, for example, in the study of the photodisintegration of the α-particle by Flower and Mandl [2]. Since then, the interest in the few-body systems continued unabated. There are several reasons for this, the main ones being: First, one may consider the few-body problem as a doorway to the many-body problem. Second, the study of the dynamics of few-nucleon systems provides us with the details about the characteristics

of the nucleon-nucleon interaction. For example, the off-shell effects can only be tested in reactions involving more than two nucleons. Third, in treating few-body systems, exact equations can be used. This in turn implies that reliable conclusions on the underlying fundamental dynamics can be drawn. However, having exact equations, one requires also rigorous computational techniques which can be used in a variety of other fields of physics as well.

A nuclear system is a many-body problem described by the many-body Schrödinger equation the solution of which can only be achieved by making drastic approximations. Unfortunately, these approximations are model dependent and can severely influence the many-body dynamics of the system. Therefore, it is desirable to use a formalism which removes as many ambiguities as possible especially in investigations concerning medium-light nuclear systems.

The simplest nuclear systems that exhibits the many-body features are the three-body and four-body systems where the particles themselves may be composites. Although the three-body is the simplest system having many-body characteristics, its direct solution from the Schrödinger equation is not straightforward, since one has to solve a six-dimensional equation, which is an intractable problem. Furthermore, the momentum space kernels associated with the three-body equations are non-compact, since they contain delta functions in their structure. The non-compactness of the kernels in turn means the solutions are not unique. As a result of the aforementioned difficulties a direct solution of the three-body Schrödinger equation remained illusive until the pioneering work of Faddeev [3].

Faddeev's idea consists of decomposing the three-body transition matrix into a sum of

channel transition matrices of two-body subsystems, commonly called Faddeev amplitudes. The work of Faddeev was taken further in a very transparent way by Sandhas and collaborators who obtained the so-called Alt-Grassberger-Sandhas (AGS) equations in momentum space [4, 5, 6]. Using the pole dominance in transitions the AGS equations reduce, after angular momentum decomposition, to a set of coupled two-variable integral equations. Thus, the Faddeev reformulation of the three-body Schrödinger equation is equivalent to converting the equations into a set of solvable multiple-scattering equations. These equations are of the Fredholm-type and thus amenable to a numerical solution. Moreover, in the case of separable interactions, the AGS equations become, after the partial wave decomposition, one-variable integral equations, and this facilitates a numerical solution considerably.

In the period immediately after Faddeev's formulation, the integral equations in momentum space were mainly the mathematically correct equations enabling to the solution of the three-body quantum problem. In order to solve these integral equations, however, one has to obtain first the two-body t-matrix for the subsystem which is needed as input into the three-body calculations and one is usually forced to make approximations at the two-body level before even attempting to solve the three-body problem. In addition, the kernel of the three-body integral equation contains the famous logarithmic singularities. Although these singularities can, nowadays, be handled numerically, an alternative approach that avoids this is desirable. Such an approach is the configuration space Faddeev method, which we discuss next.

Soon after Faddeev's *annus mirab'ilis* [3], the applicability of the configuration space Faddeev equations was considered [7, 8, 9]. Of course the need for configuration space equations of motion was recognized much earlier because our physical insight and

intuition are greatest there. However, the development towards the configuration space Faddeev equations was hampered by the lack of a proper inclusion of the boundary conditions which are automatically included in the momentum space formalism. In a series of papers by Merkuriev and co-workers [10, 11, 12, 13, 14], and the Grenoble group [15, 16, 17, 18], the configuration space Faddeev equations were put, eventually, at an equal footing with their momentum space counterparts.

The use of configuration space makes the solution of the Faddeev equations for bound states straight forward. In particular, for local potentials, after the angular momentum analysis, one uses as input for the three-body problem only two-body potentials. Nevertheless, it must be pointed out that the difficulties associated with the famous momentum space logarithmic singularities are just shifted onto the wave function asymptotics. A proper inclusion of the boundary conditions in configuration space calculations is crucial, although for bound state calculations the problem is rather simple. One only demands that the wave function be regular in the origin, and vanish asymptotically in the space outside the potential region. For the scattering case on the other hand, the situation is not as simple. Nevertheless we mention that the boundary conditions can be implemented even there for a certain class of potentials (see e.g. [14], [19], and [20]). Once the boundary conditions are correctly incorporated, a numerical solution is then possible.

There exist several methods for solving configuration space Faddeev equations, which for S-projected potentials are sometimes referred to as Noyes-Fiedeldey equations [21]. One of the early successes in the application of the configuration space Faddeev calculations is due to the works of Laverne and Gignoux [15, 16, 18]. In these calculations the binding energy of the triton obtained, using the then most realistic two-body interac-

tions of Reid [22], was found to be in better agreement with experiment as compared to other prevailing calculations at the time [23, 24, 25]. Soon afterwards the configuration space three-body scattering problem was also solved [14, 26].

In spite of the successes mentioned above, there remain some open questions. For example, all calculations with pairwise acting potentials, yield an underbinding for both the triton and ^{3}He, relative to the experimental values [15, 27, 28]. The discrepancy with experiment for the charge form factors and the charge radii for these systems is also striking [29, 30, 31]. The problem of underbinding is mainly attributed to the neglect of relativistic effects and the exclusion of three-body forces in calculations.

Another problem exists, namely, at a practical level a huge number of partial waves is needed in order to achieve convergence in the numerics. For instance, for the simple triton system 34 channels are needed to reach convergence in binding energy [30]. Clearly, the number of channels increases tremendously for systems with more structure and for more repulsive forces, and thus the handling of the corresponding equations becomes a formidable task. This is especially true in molecular systems where the van der Waals forces have a practically hard repulsive core and a weak attractive well, and therefore the calculations become not only cumbersome but also unstable, and the question of whether sufficient number of partial waves are included or not is always present. In addition, when photo- and electro-disintegration processes are considered, the construction of the wave functions using all these multitudes of partial waves results in huge numerical problems.

The question of the inclusion of partial waves can be circumvented if the Faddeev equations could be solved directly as three-dimensional equations. Already, more than

a decade ago, Kostrykin and co-workers [32] realized the merit of this and developed a three-dimensional algorithm for solving configuration space Faddeev equations known as total-angular-momentum representation method. In this thesis we use a numerical method based on collocation and on Kostrykin method, together with the tensor factorization method of Schellingerhout and co-workers [33, 34, 35, 36, 37] to give a robust method that is easily amenable to numerical application. The method is exact in the sense that it solves the Faddeev equations without resorting into the partial wave expansion. We mention here that similar three-dimensional methods in momentum space, were also considered [38, 39, 40].

One of the objectives of this work is to perform three-body bound state calculations for the weakly bounded molecular systems with a plethora of states lying close to one another. One such system is, for example, the Ozone molecule. The calculation of spectra for such systems is, generally speaking, a formidable task. There are two main reasons for this which are related to the nature of the interatomic forces. Firstly, as mentioned above already, the high repulsive interaction implies that a lot of partial waves are needed to achieve convergence. The other reason stems from the fact that the wave functions stretch over to very large distances far beyond the range of the potential. This means huge grid spaces are required in calculations. Therefore the development of good numerical methods will pave the way to study the rich underlying physics for the triatomic molecular systems. In contrast to the few-nucleon systems, molecular systems may have a large number of bound states stemming from various configurations (rotational, vibrational, etc). A question then arises as to how suitable the Faddeev-type equations in handling such systems are, i.e. by using only three-body Hamiltonian and the dominance of the pairwise forces.

Our first test case of the aforementioned momentum space method is in the application to astrophysical processes. In this respect we utilize the method to obtain the wave functions necessary to compute quantities of astrophysical interest such as reaction rates for three-body collisions, which in turn are useful in the understanding of the abundance of light elements in the universe. In the present thesis, we address the reaction rate of the $p - n$ collision in the presence of an electron, i.e. we consider a three-particle collision.

Our second test case is the three nucleon case, where we employ the commonly used Malfliet-Tjon local potentials [41, 42], and the more realistic Urbana potential [43, 44]. As a second nuclear system, we consider ^{6}Li nucleus, treated as a three-body system of an alpha nucleus, a proton, and a neutron in an isospin suppressed model. It should be noted that both cases were treated as bosonic cases as our ultimately goal was the treatment of triatomic molecular systems which are bosonic. Furthermore, in the triton case there are a lot of results to compare with the ones obtained using the three-dimensional calculations, and specifically trained finite element methods. Moreover, in the case of ^{6}Li where deep unphysical bound states exist a supersymmetric (SUSY) transformation can be used to obtain shallow potentials having $\sim 1/r^2$ singularity at the origin. The latter implies that to obtain the three-body bound state many more partial waves are needed in the calculation. This can be avoided by using exact calculations without resorting to a partial wave decomposition.

In calculations involving molecular clusters the inclusion of the three-body forces may become indispensable. For example, in some clusters it was found that three-body force effects contribute as much as 20% of the binding energy, and even as much as 50% to the virial coefficient in Argon for example [45]. In this thesis we investigate

molecular trimers of ^{4}He, and Ozone.

The exposition of this thesis is organized as follows. In Chapter 2 we describe the aforementioned three-dimensional method for solving Faddeev-type equations for a general three-cluster system in configuration-space. In particular, the total-angular-momentum representation which is the basis for these three-dimensional equations, is discussed. In addition, the boundary conditions, as well as the description on the inclusion of three-body forces in the Faddeev formalism are also, albeit briefly, discussed. The presentation of the numerical methods is given in Chapter 3. Here, apart from the discussion on the reduction of the equations to an eigenvalue problem, we also highlight some points regarding the implementation of the algorithm, such as the choice of grids and basis functions employed. In Chapter 4 we obtain reaction rates for the non-radiative process $e^- + n + p \to d + e^-$. In Chapter 5 we discuss and present the application of the configuration space method to nuclear systems whilst in Chapter 6 to molecular systems. The emphasis in Chapter 5 is on the testing of the numerics, whereas in Chapter 6 it is on the application of the methods on the more demanding molecular systems. Our conclusions and discussion, as well as future research paths, are summarized in Chapter 7.

Chapter 2

Formalism

The objective of this chapter is to outline the formalism for three-body bound state Faddeev equations in configuration space. In particular, we consider the Faddeev equations within the framework of the total angular momentum representation [32]. In this representation the Hamiltonian of the complete three-body problem is reduced to the subspace of states corresponding to a fixed total angular momentum of the system. The consequence of this reduction is that the intrinsic space of the three-particle system becomes three-dimensional in the center-of-mass system, and thus the equations become amenable to a numerical solution. The formal side of the exposition of the formalism begins with definition of the Jacobi coordinates that describe the intrinsic space.

2.1 Jacobi Coordinates

We consider a system of three particles in configuration space defined by the set of vectors $X = \{\mathbf{x}_\alpha, \mathbf{y}_\alpha\} \in \mathbb{R}^6$ $(\alpha = 1, 2, 3)$. The vectors $\mathbf{x}_\alpha$ and $\mathbf{y}_\alpha$ are the Jacobi coordinates, shown in Figure 2.1, and are expressed solely in terms of the particle coordinates $\mathbf{r}_i \in \mathbb{R}^3$ and masses m_i $(i = 1, 2, 3)$ as [3]

$$\mathbf{x}_\alpha = \left[\frac{2m_\beta m_\gamma}{m_\beta + m_\gamma}\right]^{1/2} (\mathbf{r}_\beta - \mathbf{r}_\gamma) \tag{2.1}$$

$$\mathbf{y}_\alpha = \left[\frac{2m_\alpha(m_\beta + m_\gamma)}{m_\alpha + m_\beta + m_\gamma}\right]^{1/2} \left(\mathbf{r}_\alpha - \frac{m_\beta \mathbf{r}_\beta + m_\gamma \mathbf{r}_\gamma}{m_\beta + m_\gamma}\right) . \tag{2.2}$$

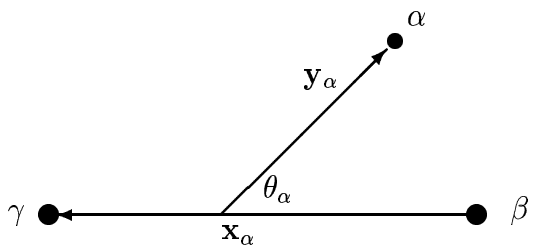

Figure 2.1: The three-body Jacobi coordinates in configuration space.

The different Jacobi coordinates are related to each other via an orthogonal transformation in $\mathbb{R}^6$ as [32]

$$\begin{pmatrix} \mathbf{x}_\beta \\ \\ \mathbf{y}_\beta \end{pmatrix} = \begin{pmatrix} C^{11}_{\beta\alpha} & C^{12}_{\beta\alpha} \\ \\ C^{21}_{\beta\alpha} & C^{22}_{\beta\alpha} \end{pmatrix} \begin{pmatrix} \mathbf{x}_\alpha \\ \\ \mathbf{y}_\alpha \end{pmatrix} \tag{2.3}$$

where the coefficients $C^{ij}_{\beta\alpha}$ are functions of the masses of the particles, given by

$$C^{11}_{\beta\alpha} = \sqrt{\frac{m_\beta m_\alpha}{(m_\alpha + m_\gamma)(m_\beta + m_\gamma)}}\,, \tag{2.4}$$

and

$$C^{12}_{\beta\alpha} = (-1)^{\alpha-\beta}\mathrm{sign}(\alpha-\beta)\sqrt{\frac{m_\gamma(m_\alpha + m_\beta + m_\gamma)}{(m_\alpha + m_\gamma)(m_\beta + m_\gamma)}} \tag{2.5}$$

with $C^{22}_{\beta\alpha} = C^{11}_{\beta\alpha}$ and $C^{21}_{\beta\alpha} = -C^{12}_{\beta\alpha}$. For three identical particles we have

$$C^{11}_{\beta\alpha} = C^{22}_{\beta\alpha} = \frac{1}{2}\,, \qquad \text{and} \qquad C^{12}_{\beta\alpha} = -C^{21}_{\beta\alpha} = \frac{\sqrt{3}}{2}\,. \tag{2.6}$$

The pairs $(\mathbf{x}_\alpha, \mathbf{y}_\alpha)$, for example, determine the six-dimensional vectors $X \in \mathbb{R}^6$,

$$X = \{|\mathbf{x}_\alpha|, |\mathbf{y}_\alpha|, \theta_\alpha, \zeta_\alpha, \vartheta_\alpha, \varphi_\alpha\}\,, \qquad \alpha = 1,2,3\,, \tag{2.7}$$

where the set $\omega \equiv (\zeta_\alpha, \vartheta_\alpha, \varphi_\alpha)$ denotes the Euler angles parameterizing a rotation of the triangle formed by the three particles, and θ_α is the angle between the Jacobi coordinates $\mathbf{x}_\alpha$ and $\mathbf{y}_\alpha$.

2.2 Configuration Space Faddeev Equations

The Schrödinger equation for three bound particles reads

$$\mathrm{H}\Psi_{3\mathrm{B}} = E_{3\mathrm{B}}\Psi_{3\mathrm{B}}\,. \tag{2.8}$$

In the presence of two-body forces (we omit at the moment three-body forces which will be introduced later) the Hamiltonian H may be written as

$$\mathrm{H} = \mathrm{H}_0 + \sum_\alpha v^{(2\mathrm{B})}_\alpha(\mathbf{x}_\alpha)\,, \qquad \alpha = 1,2,3\,, \tag{2.9}$$

where H_0 is the free three-body Hamiltonian and $v_\alpha^{(2\mathrm{B})}$ represents the two-body force. In the configuration space defined by the Jacobi coordinates $(\mathbf{x}_\alpha, \mathbf{y}_\alpha)$, the unperturbed Hamiltonian H_0 is written as

$$\mathrm{H}_0 = -\Delta_{\mathbf{x}_\alpha} - \Delta_{\mathbf{y}_\alpha} \,. \tag{2.10}$$

In order to obtain a solution, the wave function $\Psi_{3\mathrm{B}}$ is decomposed, according to the Faddeev's idea [3], into a sum of three components Φ_α $(\alpha = 1, 2, 3)$ as follows

$$\Psi_{3\mathrm{B}} = \Phi_1(\mathbf{x}_1, \mathbf{y}_1) + \Phi_2(\mathbf{x}_2, \mathbf{y}_2) + \Phi_3(\mathbf{x}_3, \mathbf{y}_3) \tag{2.11}$$

where a component $\Phi_\alpha(\mathbf{x}_\alpha, \mathbf{y}_\alpha)$ describes the two-body subsystem (β, γ) in which particle α is a spectator. Substituting Eq. (2.11) into Eq. (2.8) and using Eq. (2.9) one obtains a set of coupled differential equations

$$\Big[\mathrm{H}_0 + v_\alpha^{(2\mathrm{B})}(\mathbf{x}_\alpha) - E_{3\mathrm{B}}\Big]\Phi_\alpha(\mathbf{x}_\alpha, \mathbf{y}_\alpha) = -v_\alpha^{(2\mathrm{B})}(\mathbf{x}_\alpha) \sum_{\beta\neq\alpha} \Phi_\beta(\mathbf{x}_\beta, \mathbf{y}_\beta) \,. \tag{2.12}$$

These are the so-called configuration space Faddeev equations, and as they stand, are six-dimensional. The huge dimension makes a direct numerical solution very difficult. This problem can be circumvented, however, by considering the equations in the total-angular-momentum framework, which we discuss in the next paragraph.

2.3 Total-angular-momentum representation

For three-particle systems interacting via spherically symmetric two-body forces, the Hamiltonian commutes with the total orbital angular momentum, and one of its projection. This permits the separation of variables describing the rotation of the system

as a whole from the intrinsic variables defined by the size of the triangle formed by the three-particles. To this end the Faddeev component Φ is expanded in terms of the Wigner functions $\mathcal{D}^L_{\alpha M_L M}(\zeta_\alpha, \vartheta_\alpha, \varphi_\alpha)$ (i.e. eigenfunctions of the total angular momentum L) as follows [32, 46]

$$\Phi_\alpha(\mathbf{x}_\alpha, \mathbf{y}_\alpha) = \sum_{L, M_L, M} \frac{\phi^L_{\alpha M_L M}(x_\alpha, y_\alpha, z_\alpha)}{x_\alpha y_\alpha} \mathcal{D}^L_{\alpha M_L M}(\zeta_\alpha, \vartheta_\alpha, \varphi_\alpha)\,, \tag{2.13}$$

where $\phi^L_\alpha(x_\alpha, y_\alpha, z_\alpha)$ are the projections of the Faddeev component on subspaces with a fixed angular momentum, and x_α, y_α are the magnitudes of the Jacobi vectors, i.e. $x_\alpha = |\mathbf{x}_\alpha|$, etc., and

$$z_\alpha = \frac{(\mathbf{x}_\alpha, \mathbf{y}_\alpha)}{x_\alpha y_\alpha}\,, \qquad z_\alpha \in (-1, 1)\,. \tag{2.14}$$

The corresponding projected free Hamiltonian is

$$\mathrm{H}^L_0 = \mathcal{D}^L(g_\alpha^{-1}) x_\alpha y_\alpha \mathrm{H}_0 \frac{1}{x_\alpha y_\alpha} \mathcal{D}^L(g_\alpha)\,, \tag{2.15}$$

where g_α stands for the coordinates describing the angular motion of the system. Substituting Eq. (2.13) into Eq. (2.12) and using Eqs. (2.11) one obtains

$$\left[\mathrm{H}^L_0 + v^{(2\mathrm{B})}_\alpha(x_\alpha) - E_{3\mathrm{B}}\right] \phi^L_\alpha(x_\alpha, y_\alpha, z_\alpha) = -v^{(2\mathrm{B})}_\alpha(x_\alpha) \sum_{\beta \neq \alpha} \phi^L_\beta(x_\beta, y_\beta, z_\beta)\,. \tag{2.16}$$

These equations are the Faddeev equations in the total-angular-momentum representation. They describe three-body states with fixed total angular momentum L. This yields a set of $6L + 3$ coupled three-dimensional partial differential equations [47].

In terms of the intrinsic coordinates, x_α, y_α, and z_α, the projected free Hamiltonian, for the case $L = 0$ which we consider from here onwards, reads

$$\mathrm{H}^0_0 = -\frac{\partial^2}{\partial x^2_\alpha} - \frac{\partial^2}{\partial y^2_\alpha} - \left(\frac{1}{x^2_\alpha} + \frac{1}{y^2_\alpha}\right) \frac{\partial}{\partial z_\alpha}(1 - z^2_\alpha) \frac{\partial}{\partial z_\alpha}\,. \tag{2.17}$$

In the case where the particles are identical a simple relationship between the different projected Faddeev components in (2.16) exists. More specifically

$$\phi^0_\beta(x_\beta, y_\beta, z_\beta) = P^+ \phi^0_\alpha(x_\alpha, y_\alpha, z_\alpha)\,, \tag{2.18}$$

$$\phi^0_\gamma(x_\gamma, y_\gamma, z_\gamma) = P^- \phi^0_\alpha(x_\alpha, y_\alpha, z_\alpha)\,, \tag{2.19}$$

where P^+ (P^-) is the cyclic (anticyclic) permutation operator acting on the coordinates. The result of operating on the Faddeev components with operators $P^\pm$ is

$$P^+\phi^0(x,y,z) = xy\frac{\phi^0(x^+,y^+,z^+)}{x^+y^+} \tag{2.20}$$

$$P^-\phi^0(x,y,z) = xy\frac{\phi^0(x^-,y^-,z^-)}{x^-y^-}\,, \tag{2.21}$$

where the now redundant subscript α has been dropped. The permuted coordinates $x^\pm(x,y,z)$, $y^\pm(x,y,z)$, $z^\pm(x,y,z)$ are given by

$$x^\pm(x,y,z) = \left(\frac{1}{4}x^2 + \frac{3}{4}y^2 \mp \frac{\sqrt{3}}{2}xyz\right)^{1/2} \tag{2.22}$$

$$y^\pm(x,y,z) = \left(\frac{3}{4}x^2 + \frac{1}{4}y^2 \pm \frac{\sqrt{3}}{2}xyz\right)^{1/2} \tag{2.23}$$

$$z^\pm(x,y,z) = \frac{\pm\frac{\sqrt{3}}{4}x^2 \mp \frac{\sqrt{3}}{4}y^2 - \frac{1}{2}xyz}{x^\pm(x,y,z)y^\pm(x,y,z)}\,. \tag{2.24}$$

Substitution of Eqs. (2.18) and (2.19) into (2.16), reduces the latter to a single equation

$$\Big[\mathrm{H}^0_0 + v^{(2\mathrm{B})}(1 + P^+ + P^-) - E_{3\mathrm{B}}\Big]\phi^0(x,y,z) = 0\,. \tag{2.25}$$

Throughout in this thesis we consider the simpler and the most interesting case where the total angular momentum is zero, i.e. the equations we solve in our investigations are (2.25). We shall also from now on drop the superscript corresponding to the quantum number L.

2.4 Boundary Conditions

To obtain a unique solution to the differential Faddeev equations (2.25) one must supplement them with the relevant boundary conditions. More specifically, in the case where only one bound state in each two-body subsystem is sustained, the asymptotic behaviour of the Faddeev component is a sum of two terms, namely, the (2+1)-configuration and the (1+1+1)-configuration. That is [48]

$$\phi(x,y,z) \quad \sim \quad \varphi_{2\mathrm{B}}(x)\exp\{-\sqrt{E_{2\mathrm{B}}-E_{3B}}\,y\}+\mathcal{A}\frac{\exp\{-\sqrt{-E_{3\mathrm{B}}(x^2+y^2)}\}}{(x^2+y^2)^{1/4}}\,, \tag{2.26}$$

where $\varphi_{2\mathrm{B}}$ is the two-body bound state in the two-body subsystem, $E_{2\mathrm{B}}$ the corresponding energy, and $E_{3\mathrm{B}}$ is the energy of the three-body system, whilst $\mathcal{A}$ is the scattering amplitude. The term corresponding to the (1+1+1)-configuration decreases much faster than the (2+1)-configuration term and can be neglected for sufficiently large distances. Thus the asymptotic boundary conditions for ϕ read

$$\phi(x,y,z) \quad \sim \quad \varphi_{2\mathrm{B}}(x)\exp\{-\sqrt{E_{2\mathrm{B}}-E_{3B}}\,y\}\,. \tag{2.27}$$

Furthermore, the $\varphi_{2\mathrm{B}}$ behaves asymptotically as

$$\varphi_{2\mathrm{B}}(x)\sim\exp\{-\sqrt{E_{2\mathrm{B}}}\,x\}\,. \tag{2.28}$$

Hence, for sufficiently large distances $x_{\max}$ and $y_{\max}$, the asymptotic boundary conditions for the Faddeev component ϕ are simplified to

$$\frac{\partial\phi}{\partial x}\ln\phi(x,y,z)\Big|_{x=x_{\max}} \quad = \quad -\sqrt{E_{2\mathrm{B}}}\,, \tag{2.29}$$

$$\frac{\partial\phi}{\partial y}\ln\phi(x,y,z)\Big|_{y=y_{\max}} \quad = \quad -\sqrt{E_{2\mathrm{B}}-E_{3\mathrm{B}}}\,. \tag{2.30}$$

In addition ϕ must satisfy the regularity conditions

$$\phi(x,y,z)\Big|_{x=0,\infty} = 0 \tag{2.31}$$

$$\phi(x,y,z)\Big|_{y=0,\infty} = 0\,. \tag{2.32}$$

For more rigorous description of the boundary conditions for three-body systems see, for example, Ref. [19].

2.5 Inclusion of Three-Body Forces

The inclusion of three-body interactions can in principle be done by simply adding the three-body force to the two-body force on the left-hand side of the Faddeev equations, so that the corresponding equations read

$$\Big[\mathrm{H}_0 + v_\alpha^{(2\mathrm{B})}(x_\alpha) + \mathcal{V}^{(3\mathrm{B})} - E_{3\mathrm{B}}\Big]\Phi_\alpha(x_\alpha,y_\alpha,z_\alpha) = -v_\alpha^{(2\mathrm{B})}(x_\alpha)\sum_{\beta\neq\alpha}\Phi_\beta(x_\beta,y_\beta,z_\beta)\,, \tag{2.33}$$

where $\mathcal{V}^{(3\mathrm{B})}$ is the three-body force and $v^{(2\mathrm{B})}$, as before, represents the two-body force. We mention in passing that the inclusion of three-body force according to (2.33) is valid within the framework of perturbation theory.

From a numerical point of view, the inclusion of three-body force in the Hamiltonian raises an interesting and pertinent question, namely: Should the three-body force be retained on the left-hand side of the Faddeev equations or be transferred to the right hand-side, in order to facilitate convergence in calculations? This question is pertinent since the coupled Faddeev equations, in their original form, were derived with short-range interactions. It is therefore of interest to ask whether this coupling is preserved

when the three-body force is included. There are several possibilities on the handling of this question, depending on the structure of the three-body force itself. For instance, one may add the three-body term $\mathcal{V}^{(3B)}$ to the two-body potential terms on the right-hand side of the equations and regroup terms as follows [49]

$$v_\beta^{(2B)} + v_\gamma^{(2B)} + \mathcal{V}^{(3B)} = \left(v_\beta^{(2B)} + \frac{1}{2}\mathcal{V}^{(3B)}\right) + \left(v_\gamma^{(2B)} + \frac{1}{2}\mathcal{V}^{(3B)}\right) . \tag{2.34}$$

This decomposition leads to the set of coupled Faddeev equations

$$\left[\mathrm{H}_0 + v_\alpha^{(2B)} - E_{3B}\right]\Phi_\alpha = -\left(v_\alpha^{(2B)} + \frac{1}{2}\mathcal{V}^{(3B)}\right)\sum_{\beta\neq\alpha}\Phi_\beta . \tag{2.35}$$

Yet another possibility arises when the three-body force itself is such that it can be split into three components as follows [30, 49]

$$\mathcal{V}^{(3B)} = \sum_{\gamma'=\alpha,\beta,\gamma} U_{\gamma'}^{(3B)} , \tag{2.36}$$

where the $U_i^{(3B)}$ have the same functional form but cyclically permuted coordinates. This decomposition leads in a natural way to a grouping of the pairwise interaction $v_\alpha^{(2B)}$ together with the three-body component $U_\alpha^{(3B)}$, both of which are symmetric under the exchange of particles β and γ. For this case the Faddeev coupled equations are

$$\left[\mathrm{H}_0 + v_\alpha^{(2B)} + U_\alpha^{(3B)} - E_{3B}\right]\Phi_\alpha = -\left(v_\alpha^{(2B)} + U_\alpha^{(3B)}\right)\sum_{\beta\neq\alpha}\Phi_\beta . \tag{2.37}$$

We mention that decomposition (2.36) is a natural one for a two-pion exchange three-nucleon force. In this notation, $U_\alpha^{(3B)}$ represents a process in which particle α exchanges one pion with each of particles β and γ, shown pictorially in Figure 2.2.

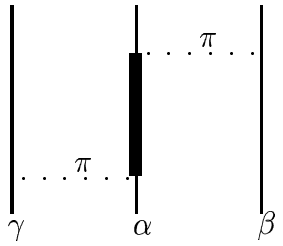

Figure 2.2: A Feynman diagram illustrating a two-pion exchange nuclear three-body force U_α. Thick line represents an isobar.

On the other hand, molecular three-body forces are not separable according to decomposition (2.36), in general. This is the case, for example, of the long-range three-body interaction of Axilrod-Teller-Muto (ATM) type [50, 51],

$$\mathcal{V}^{(3B)} = C\frac{1+3\cos\theta_\alpha\cos\theta_\beta\cos\theta_\gamma}{(r_\alpha r_\beta r_\gamma)^3}\,, \tag{2.38}$$

where C is a constant characteristic of a system, and the coordinates r_i, θ_i, $(i=\alpha,\beta,\gamma)$ are sides and internal angles of the triangle formed by the three atoms making up the system as shown in Figure A.1. To be explicit, the lowest graph in perturbation theory corresponding to (2.38), i.e. the triple-dipole three-body force of rare gases, is shown in Fig. 2.3, which is clearly nonseparable. In this case, one has to include the three-body potential on the left hand side of the Faddeev equations.

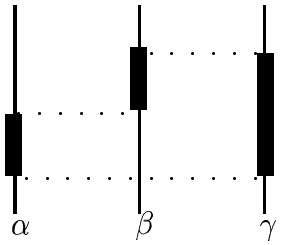

Figure 2.3: A Feynman diagram illustrating the lowest graph corresponding to, e.g. the triple-dipole three-body force of rare gases.

Chapter 3

Numerical Methods

In the present chapter we discuss the numerical method used to solve the configuration space Faddeev equations, given in the previous chapter. The described method is suitable for both the nuclear three-body bound state calculations, and for the more demanding molecular calculations where the potential is, for all practical purposes of a hard core nature.

3.1 Reduction to an Eigenvalue Problem

Our aim is to obtain the regular solution of Eq. (2.25), subject to the boundary conditions (2.27) – (2.32). To this end we approximate the solution by an expansion in

terms of a set of L^2-integrable basis functions as follows [28, 33, 52]

$$\Phi(x,y,z) = \sum_{l=1}^{L}\sum_{m=1}^{M}\sum_{n=1}^{N} \mathcal{C}_{lmn} \mathrm{S}_l(x)\mathrm{S}_m(y)\mathrm{S}_n(z) \ . \tag{3.1}$$

where the subscripts L, M and N refer to the number of basis functions in the three variables (x,y,z), respectively, while the basis functions S′s themselves are chosen in this work to be the piecewise quintic Hermite splines.

Substitution of Eq. (3.1) into Eq. (2.25), followed by the orthogonal collocation procedure described in Ref. [28], results – in the presence of two-body forces only – in a system of linear algebraic equations for the expansion coefficients $\mathcal{C}$

$$[\hat{\mathrm{H}}_0 + \hat{v}^{(2\mathrm{B})} + \hat{v}^{(2\mathrm{B})}(\hat{P}^+ + \hat{P}^-) - E_{3\mathrm{B}}\hat{I}]\mathcal{C} = 0 \ , \tag{3.2}$$

where a hat on the operator indicates a discrete analog of the corresponding operator in Eq. (2.25) and $\hat{I}$ is a unit matrix. We may rewrite (3.2) in the form

$$[\hat{\mathrm{H}}_1 + \hat{\mathrm{H}}_2 - E_{3\mathrm{B}}\hat{I}]\mathcal{C} = 0 \ , \tag{3.3}$$

where the hamiltonians $\hat{\mathrm{H}}_1$ and $\hat{\mathrm{H}}_2$ are

$$\hat{\mathrm{H}}_1 = \hat{\mathrm{H}}_0 + \hat{v}^{(2\mathrm{B})} \, , \tag{3.4}$$

$$\hat{\mathrm{H}}_2 = \hat{v}^{(2\mathrm{B})}(\hat{P}^+ + \hat{P}^-) \, . \tag{3.5}$$

Two remarks should be passed concerning equation (3.3). First, the matrices involved are huge. Second, the equation is in general ill-conditioned and standard iterative methods are difficult to apply. Treating $E_{3\mathrm{B}}$ as a parameter, Eq. (3.3) can be turned into an eigenvalue equation

$$-(\hat{\mathrm{H}}_1 - E_{3\mathrm{B}}\hat{I})^{-1}\hat{\mathrm{H}}_2\mathcal{C} = \Lambda\mathcal{C} \, , \tag{3.6}$$

where Λ is the eigenvalue corresponding to the energy $E_{3\mathrm{B}}$. Clearly, eigenvalues with $\Lambda = 1$ correspond to physical solutions whereby $E_{3\mathrm{B}}$ is a three-body binding energy.

In view of the aforementioned discussion, the problem of calculating the eigensolutions to Eq. (2.25) now reduces to that of finding the discrete spectrum of the Faddeev operator

$$\hat{\mathcal{F}} = -(\hat{\mathrm{H}}_1 - E_{3\mathrm{B}}\hat{I})^{-1}\hat{\mathrm{H}}_2\,. \tag{3.7}$$

Hence, it follows that the eigenvalue problem (3.6), which may be rewritten as

$$\hat{\mathcal{F}}\mathcal{C} = \Lambda\mathcal{C}\,, \tag{3.8}$$

can now be solved via standard methods for large matrices such as Lanczos and Arnoldi. As discussed in Ref. [53], the above procedure is satisfactory for a wide range of potentials. However, for interatomic potentials which are for all practical purposes of hard-core nature, several problems are encountered, of which the two main ones are: First, the spectrum contains numerous large negative eigenvalues. Second, there are several eigenvalues close to one. These features make the convergence tremendously slow and numerically unstable. The large number of negative eigenvalues suppresses the convergence of the Arnoldi algorithm. The existence of several eigenvalues close to one renders it difficult to pinpoint a physical solution, i.e. an eigenvector corresponding to $\Lambda = 1$.

There are several steps that can be taken to address the convergence problems mentioned above. For example, as pointed out in [53], the large number of negative eigenvalues that suppress convergence can be eliminated from the spectrum by considering instead of the operator $\hat{\mathcal{F}}$ the spectrum of the operator

$$\hat{\mathcal{M}}(z) = (\hat{\mathrm{H}}_0 + \hat{V} + \hat{V}_m - z)^{-1}(\hat{V}_m - \hat{V}\hat{P})\,, \tag{3.9}$$

where $\hat{V}_m$ is the so-called modifying potential. It can be shown that the positive eigenvalues of $\hat{\mathcal{M}}$ in the vicinity of 1 are identical to those of $\Lambda_{i,\mathcal{F}} = 1$ and are independent of the modifying potential. On the other hand, however, the negative eigenvalues – which are eigenvalues of the equation

$$[\hat{\mathrm{H}}_0 + 2\hat{V}_m + \hat{V}(1 - \hat{P}) - z_i]\mathcal{C} = 0\,, \tag{3.10}$$

depend on the modifying potential $\hat{V}_m$ and can be eliminated by a proper choice of $\hat{V}_m$. According to Arnoldi algorithm convergence estimations this feature of $\hat{\mathcal{M}}$ should improve dramatically the convergence of the eigenvalues. A further improvement on convergence rate can be achieved by using instead of $\hat{\mathcal{M}}(z)$, an even power of $\hat{\mathcal{M}}(z)$ in spectral calculations [53]. This technique increases the separation between the physically interesting eigenvalues close to one and the rest of the spectrum. These various features mentioned above, put together, lead to a reduction in computation time and memory requirements.

Yet another simplification towards a tractable numerical solution, lies in exploiting the tensor structure of the matrices of Eq. (3.3). The whole procedure of exploiting the tensor structure of the matrices is nowadays known as tensor-trick [33]. For example, the matrix $\hat{\mathrm{H}}_1$ in Eq. (3.4), has a tensor structure of the form

$$\begin{aligned}
\hat{\mathrm{H}}_1 &= \hat{D}_x \otimes \hat{S}_y \otimes \hat{S}_z \;+\; \hat{S}_x \otimes \hat{D}_y \otimes \hat{S}_z \\
&+ \;\; \hat{S}_x \otimes \hat{S}_y (\hat{\mathrm{L}}_x \otimes \hat{\mathbb{1}}_y \otimes \hat{\mathbb{1}}_z \;+\; \hat{\mathbb{1}}_x \otimes \hat{\mathrm{L}}_y \otimes \hat{\mathbb{1}}_z) \otimes \hat{D}_z \\
&+ \;\; v^{(2\mathrm{B})} \hat{S}_x \otimes \hat{S}_y \otimes \hat{S}_z \\
&\equiv \;\; \hat{\mathrm{H}}_1^0 \otimes \hat{I} + \hat{I} \otimes v^{(2\mathrm{B})}
\end{aligned} \tag{3.11}$$

where $\hat{D}_t$, $\hat{S}_t$ and $\hat{\mathbb{1}}_t$ represent respectively, the matrix of the differential-operator, identity-operator and the unit matrix in coordinate t. It is clear from (3.11) that $\hat{\mathrm{H}}_1$

is expressible as a product of matrices of smaller dimensions, which permits an easy diagonalization $\hat{\mathrm{H}}_1$ as we shall show in the next section. In conclusion we mention that the matrix $(\hat{P}^+ + \hat{P}^-)$, hence $\hat{\mathrm{H}}_2$, is sparse, and can be easily stored using standard methods for storing sparse matrices [54].

In the presence of three-body forces the corresponding equation to (3.2) reads

$$[\hat{\mathrm{H}}_0 + \hat{v}^{(2\mathrm{B})} + \mathcal{V}^{(3\mathrm{B})} + \hat{v}^{(2\mathrm{B})}(\hat{P}^+ + \hat{P}^-) - E_{3\mathrm{B}}\hat{I}]\mathcal{C} = 0 \;, \tag{3.12}$$

which leads to two possible ways of defining $\hat{\mathrm{H}}_1$ and $\hat{\mathrm{H}}_2$. The first possibility is to define $\hat{\mathrm{H}}_1$ as in the case when only two-body forces are present, according to (3.4) whilst $\hat{\mathrm{H}}_2$ is defined by

$$\hat{\mathrm{H}}_2 \;=\; \hat{v}^{(2\mathrm{B})}(\hat{P}^+ + \hat{P}^-) + \mathcal{V}^{(3\mathrm{B})} \,. \tag{3.13}$$

The second possibility is the following

$$\hat{\mathrm{H}}_1 \;=\; \hat{\mathrm{H}}_0 + \hat{v}^{(2\mathrm{B})} + \mathcal{V}^{(3\mathrm{B})} \,, \tag{3.14}$$

$$\hat{\mathrm{H}}_2 \;=\; \hat{v}^{(2\mathrm{B})}(\hat{P}^+ + \hat{P}^-) \,, \tag{3.15}$$

i.e. to retain the three-body force together with the free Hamiltonian $\hat{\mathrm{H}}_0$. The tensor structure of $\hat{\mathrm{H}}_1$ in (3.15) is, in analogy with (3.11)

$$\begin{aligned}
\hat{\mathrm{H}}_1 \;&=\; \hat{D}_x \otimes \hat{S}_y \otimes \hat{S}_z \;+\; \hat{S}_x \otimes \hat{D}_y \otimes \hat{S}_z \\
&+\; \hat{S}_x \otimes \hat{S}_y(\hat{\mathrm{L}}_x \otimes \hat{\mathbb{1}}_y \otimes \hat{\mathbb{1}}_z \;+\; \hat{\mathbb{1}}_x \otimes \hat{\mathrm{L}}_y \otimes \hat{\mathbb{1}}_z) \otimes \hat{D}_z \\
&+\; (v^{(2\mathrm{B})} + \mathcal{V}^{(3\mathrm{B})})\hat{S}_x \otimes \hat{S}_y \otimes \hat{S}_z \\
&\equiv\; \hat{\tilde{\mathrm{H}}}_1^{\,0} \otimes \hat{I} + \hat{I} \otimes \mathcal{V}^{(3\mathrm{B})}
\end{aligned} \tag{3.16}$$

where $\hat{\tilde{\mathrm{H}}}_1^{\,0}$ is equivalent to $\hat{\mathrm{H}}_1$ in (3.11). The difference between factorization (3.11) and (3.16) is the following: The computation of the tensor products in (3.16) must be done

recursively [55]

$$\begin{aligned} \hat{\mathrm{H}}_1 &= \hat{\mathrm{H}}_1^0 \otimes \hat{I} + \hat{I} \otimes \mathcal{V}^{(3\mathrm{B})}\,, \\ \hat{\mathrm{H}}_1^0 &= [\hat{D}_x + \hat{D}_y + (\hat{\mathrm{L}}_x + \hat{\mathrm{L}}_y)] \otimes \hat{I} + \hat{I} \otimes v^{(2\mathrm{B})}\,. \end{aligned} \tag{3.17}$$

In general, for n independent variables, the recursive tensor product representation for a matrix $\mathcal{F}$ has the form [55]

$$\begin{aligned} \mathcal{F} &= C_1 \otimes B_1 + I \otimes A_1\,, \\ C_1 &= C_2 \otimes B_2 + I \otimes A_2\,, \\ \vdots &\qquad \ddots \qquad\quad \ddots \\ C_{n-2} &= C_{n-1} \otimes B_{n-1} + I \otimes A_{n-1}\,, \end{aligned} \tag{3.18}$$

where $\mathcal{F}$ itself satisfies the matrix equation of the form $\mathcal{F}u = g$.

3.2 Diagonalization of matrices

Due to the large sizes of the matrices involved, it is not easy to solve directly the eigenvalue problem (3.6). To address this we resort to the tensor-trick technique [37]. The central feature of the tensor-trick method is the determination of the inverse of the matrix operator $(\hat{\mathrm{H}}_1 - E_{3\mathrm{B}}\hat{I})$ in terms of matrices of comparatively smaller dimensions in order to facilitate computation in diagonalization. We present here the case considered in Ref. [53] with two-body forces only and we briefly recapitulate some of the salient points. To this end, we mention first that the matrices constituting the tensor product of $\hat{\mathrm{H}}_1$ are diagonally dominant, since they originate from discretization of elliptic equations. Hence there exist diagonal matrices

$$\hat{X}^i = \mathrm{diag}\{E^i_{x_1}, \cdots, E^i_{x_{N_x}}\}\,, \tag{3.19}$$

$$\hat{Y}^i = \mathrm{diag}\{E^i_{y_1}, \cdots, E^i_{y_{N_y}}\}\,, \tag{3.20}$$

$$\hat{L}_z = \mathrm{diag}\{\ell_1, \cdots, \ell_{N_z}\}\,, \tag{3.21}$$

from which the matrices $\hat{B}_z$, $\hat{B}^i_x$, $\hat{B}^i_y$ satisfying

$$(\hat{D}_x + \hat{v}^{(2\mathrm{B})}\hat{S}_x + \ell_i\hat{\mathrm{L}}_x\hat{S}_x)\hat{B}^i_x \equiv \hat{X}^i\hat{S}_x\hat{B}^i_x\,, \tag{3.22}$$

$$(\hat{D}_y + \ell_i\hat{\mathrm{L}}_y\hat{S}_y)\hat{B}^i_y \equiv \hat{Y}^i\hat{S}_y\hat{B}^i_y\,, \tag{3.23}$$

$$\hat{D}_z\hat{B}_z \equiv \hat{\mathrm{L}}_z\hat{S}_z\hat{B}_z\,, \tag{3.24}$$

can be constructed. The variables E^i_t in (3.19) – (3.20) are eigenvalues of the corresponding operators. Next we construct the matrix $\hat{B}$ as a tensor product of $\hat{B}_z$, $\hat{B}^i_x$, $\hat{B}^i_y$, as follows

$$\hat{B} \equiv \prod_{i=1}^{N_z} \oplus(\hat{B}^i_x \otimes \hat{B}^i_y) \otimes [\hat{B}_z]_i\,. \tag{3.25}$$

Clearly, the matrix product $\hat{B}^*\hat{B} = \hat{\mathbb{1}}_x \otimes \hat{\mathbb{1}}_y \otimes \hat{\mathbb{1}}_z$, i.e. an identity matrix and

$$\hat{B}^*(\hat{H}_1 - E_{3\mathrm{B}}\hat{I})\hat{B} = \hat{G}\,, \tag{3.26}$$

where $\hat{G}$ is diagonal matrix given by $\hat{G} = \mathrm{diag}\{g_{111}, g_{112}, \cdots, g_{i_x i_y i_z}, \cdots g_{N_x N_y N_z}\}$ with $g_{i_x i_y i_z}$ in turn given by $g_{i_x i_y i_z} = E^{i_z}_{xi_x} + E^{i_z}_{xi_y} - E_{3\mathrm{B}}$. Hence

$$(\hat{H}_1 - E_{3\mathrm{B}}\hat{I})^{-1} = \hat{B}\hat{G}^{-1}\hat{B}^*\,, \tag{3.27}$$

i.e. the inverse of the matrix $(\hat{\mathrm{H}}_1 - E_{3\mathrm{B}})$ can be written as a product of simpler matrices. Indeed, the matrix G is diagonal and its inverse can be trivially obtained.

The computational cost in diagonalizing the inverse of ($\hat{\mathrm{H}}_1$ - $E_{3\mathrm{B}}\hat{I}$) is determined by the operations involved in multiplication of the matrices on the right-hand side of (3.27) with a vector $\mathbf{v}$, say. To this end, we note that using the identity [53]

$$\hat{B}_x \otimes \hat{B}_y = \hat{I} \otimes \hat{B}_y\hat{B}_x \otimes \hat{I} \tag{3.28}$$

it follows that the calculation of $\hat{I} \otimes \hat{B}_y \mathbf{v}$ requires $N_x^2 N_y$ whilst that of $\hat{B}_x \otimes \hat{I} \mathbf{v}$ is $N_x N_y^2$. Therefore, the calculation of a tensor product $\hat{B}_x \otimes \hat{B}_y$ by a vector $\mathbf{v}$ would cost $(N_x^2 N_y + N_x N_y^2)$ or $N_x N_y (N_x + N_y)$. In contrast, a direct calculation of the product $\hat{B}_x \otimes \hat{B}_y \mathbf{v}$ requires $N_x^2 N_y^2$. Thus the correct implementation of a direct sum by a vector can reduce the amount of computational cost by $N_x N_y N_z / (N_x + N_y + N_z)$. This is indeed a significant reduction in the arithmetic operations required for the diagonalization of (H_1 - $E_{3\mathrm{B}} \hat{I}$). In closing we pass the following remark: our spectral problem obtained after the decomposition of the matrices, is solved by means of the Restarted Arnoldi algorithm in conjunction with Chebyshevy acceleration techniques [56, 57, 58] for solving nonsymmetric eigenvalue problems.

3.3 Optimization Methods

In cases where a plethora of closely lying states exist convergence challenges are formidable. Moreover, because of this, it may not be feasible to definitively discriminate all the levels when only a single strategy is employed. In order to address this question, i.e. the handling of a large number of closely lying states, optimization methods can be employed. Two optimization methods were used in this work. More specifically we used the MERLIN [59] optimization package, which is a direct method for a local search, and the global optimization package PANMIN [60] that relies on MERLIN. MERLIN supports many optimization algorithms. These include direct, gradient, and conjugate gradient methods. Examples of the first group of methods include the Simplex method, whereas the gradient methods include the so-called BFGS [61] update methods. For the conjugate gradient methods, we cite the Fletcher-Reeves [62] and Polak-Ribiere

[63] methods. The Levenberg-Marquardt method [64] for computing sum of squares is also incorporated within the MERLIN package. We remark that it is the combination of these strategies that makes MERLIN highly effective and robust, in contrast to, for example, library routines that implement a single algorithm.

We recall that the differential Faddeev equations can be transformed into an eigenvalue problem according to Eq. (3.8). Hence, after the discretization of the rectangular domain, the problem can be turned into a minimization problem

$$I(E_\lambda;\mathbf{p}) = \frac{\sum_i [\mathcal{F}\Psi_\lambda(x_i,y_i,z_i;\mathbf{p}) - \Lambda_\lambda(E_\lambda)\Psi_\lambda(x_i,y_i,z_i;\mathbf{p})]^2}{\sum_i [\Psi_\lambda(x_i,y_i,z_i;\mathbf{p})]^2}, \tag{3.29}$$

where the trial eigenfunction Ψ_λ is defined on the collocation points (x_i, y_i, z_i), and $\mathbf{p}$ is the parameter vector. In what follows we describe very briefly the principle in the application of the PANMIN algorithm.

For a given energy interval, say $[E_0, E_n]$, the PANMIN algorithm locates all the minima of the objective function that are potentially global. The local minima $E_0 \leq E_\lambda \leq E_n$ are obtained via a local search method, i.e. employing the MERLIN package. Using this one can calculate any number of states by projecting out from the trial wave function the already computed levels [65].

Finally, we refer to Ref. [60] and references therein for a full description of PANMIN algorithm. In addition we also point out that the optimization packages mentioned here are maintained at the site *http://merlin.cs.uoi.gr*, to which an interested reader is referred.

3.4 Algorithm Implementation

In order to perform calculations, the infinite interval on which the Faddeev equations are defined must be reduced to a finite interval. There are several ways of doing this. One way is the radius cutoff method. Another approach is the transformation of the infinite interval onto a finite interval [33]. In our calculations we employ the former approach. In the x and y coordinates in order to achieve convergence, the cutoff radii are taken to be very large compared to the ranges of the physical quantities – a pathology which stems from asymptotic boundary conditions used in solving the integrodifferential Faddeev equations [66]. The z-grid is defined differently as explained below.

In implementing the algorithm, the choice of the x-grid is very crucial since it must be optimized to reproduce the two-body binding as well. This is achieved as follows: Let $\Omega_x = [a_0, x_{\max}]$ be the domain for the x grid, where a_0 is a measure of the distance from $x = 0$ carefully chosen to eliminate numerical noise associated with the $x \to 0$ behaviour. Then we divide Ω_x into two subdomains, namely, the interior domain $\Omega_{x,I}$ and the exterior domain $\Omega_{x,J}$, separated by some carefully chosen break-point x_B. That is, we generate a partition $a_0 = x_0 < x_1 < \cdots < x_B < \cdots < x_{N_x} = x_{\max}$.

It is required that the domain $\Omega_{x,I}$ fulfill the following characteristics. First, it be relatively dense compared to $\Omega_{x,J}$. Second, it must have small separation between grid points, and thirdly it must contain a sufficient number of points to describe well the most important ranges affecting the physical quantities involved. In other words the grid must be constructed such that the density of the points is higher where the wave functions are important. For example, for bound states, the wave function has

more structure at small values of x, and thus $\Omega_{x,I}$ should cover this region of the wave function sufficiently whilst $\Omega_{x,J}$ covers the asymptotic region. It was found that a simple transformation

$$x_{i+1} = a_0 + i\delta x_i^{(I)}\,, \qquad i = 1, 2, \cdots, N_{x,I} - 1\,, \tag{3.30}$$

$$x_i = x_{i-1} + \delta x_i^{(J)}\,, \quad i = N_{x,I}, \cdots, N_x\,, \tag{3.31}$$

where the δx_i's are the scaling functions, and $N_{x,I}$ is the number of interior points in the domain $\Omega_{x,I}$, fulfills the requirements described. As a rule of thumb the break point x_B is chosen in such a way that roughly two-thirds of the x-grid points are interior points. The y-grid is defined similarly with $\Omega_{y,I}$ and $\Omega_{y,J}$ the interior- and the exterior-domain respectively. However, here a_0 is set equal to zero. In addition, the requirement that the density of the points in the interior domain be dense compared to the exterior domain may be relaxed. In practice it was found that convergence is achieved even when there are more points in the exterior domain than the interior domain. On the other hand the z-grid, $z_0 < z_1 < \cdots < z_{N_z}$, is obtained by the transformation

$$z_i = g(t_i)\,, \qquad i = 0, \cdots\cdots, N_z\,, \tag{3.32}$$

where $t_i = -1 + i\delta z$ and the function g is given by

$$g(t) = \frac{(t + C_0 t^3)}{(1 + C_0)}\,, \tag{3.33}$$

with $z_0 = -1$ and $z_{N_z} = 1$, and the control parameter is chosen within $-1 < C_0 \leq 0$. A typical value of C_0 is – 0.3333. It is to be noted that the function $g(t)$ is chosen to satisfy the condition $g(0) = 0$ and $g(1) = 1$.

Before concluding this section, the following remark in respect of the basis functions in the expansion of the Faddeev amplitudes in (3.1) is in order. We note that different

types of basis functions are available for the expansion (3.1). However, spline functions are known to offer a lot of advantages [28] compared to other polynomials and are employed in this work. In particular we employ the triquintic Hermite splines, which are known to improve the convergence considerably [67], and for completeness we write here their explicit analytical forms. The three splines $\phi_{i\sigma}$ ($\sigma = 0, 1, 2$) which are nonzero only on two adjacent subintervals $[x_{i-1}, x_i] \bigcup [x_i, x_{i+1}]$, are

$$\phi_{i\sigma}(x) = (1-\Delta)^3 (x - x_i)^\sigma \begin{cases} 6\Delta^2 + 3\Delta + 1\,, & \text{for} \quad \sigma = 0\,, \\ 3\Delta + 1\,, & \text{for} \quad \sigma = 1\,, \\ \frac{1}{2}\,, & \text{for} \quad \sigma = 2\,, \end{cases} \tag{3.34}$$

where $x \in [x_{i-1}, x_{i+1}]$, and Δ is defined by

$$\begin{aligned} \Delta &= \frac{x - x_i}{x_{i-1} - x_i}\,, x_{i-1} \le x \le x_i \\ \Delta &= \frac{x - x_i}{x_{i+1} - x_i}\,, x_i \le x \le x_{i+1}\,. \end{aligned} \tag{3.35}$$

In implementing the method we employ the orthogonal collocation method with three Gaussian quadrature points per subinterval. This means that for a basic grid with N points there are $(3N + 3)$ collocation points. Once the collocation points are obtained, the matrix elements of the operators in (2.25) are easily constructed, leading to $(3N+3)$ equations. These equations must be supplemented by the boundary conditions before a numerical solution is sort. For the coordinates x and y, collocation method supplemented by the boundary conditions (2.29) reduces the number of equations from $3N+3$ to $3N$. For the z coordinate the number remains $3N_z + 3$. Thus the dimension of the system of equations to be solved is rather large and equals $N_T = 3N_x \times 3N_y \times 3(N_z + 1)$.

Finally we pass the following remark: The implementation of the global optimization

method is achieved via an interface routine that calls the aforementioned algorithm. A further description on the use of this interface routine is given in Chapter 6.

Chapter 4

Applications I : Astrophysical Processes

One of the simplest question concerning few-body dynamics is the role played by triple collisions in primordial nucleosynthesis. In the past, calculations concerned mainly three-nucleon reactions. Comparatively little work was done focusing on astrophysical reactions at ultra-low energies which are extremely important in understanding the question of the abundance of elements in the universe. Even here, the relevant calculations were made by assuming that the reaction proceeded via two-body collisions only, while three-body collisions, which might have existed in the early age of the generation of the universe, were completely ignored. In the present chapter, we address the astrophysical three-body collision problem by considering the deuteron formation via the collision of neutron and proton in the presence of electrons.

4.1 Nucleosynthesis in Primordial Plasma

In the Standard model of Big Bang nucleosynthesis [68], it is assumed that the formation of light nuclei mainly occurs through the *pp*-chain which begins with the synthesis of deuterons via the processes

$$\mathrm{p} + \mathrm{p} \;\rightarrow\; \mathrm{d} + \mathrm{e}^{+} + \nu_{\mathrm{e}} \;, \tag{4.1}$$

$$\mathrm{p} + \mathrm{e}^{-} + \mathrm{p} \;\rightarrow\; \mathrm{d} + \nu_{\mathrm{e}} \,, \tag{4.2}$$

involving strong and weak forces, and the strong-electromagnetic reaction

$$\mathrm{n} + \mathrm{p} \rightarrow \mathrm{d} + \gamma \;. \tag{4.3}$$

The next step in the process is the radiative capture of protons by deuterons

$$\mathrm{p} + \mathrm{d} \rightarrow {}^{3}\mathrm{He} + \gamma \;. \tag{4.4}$$

Then, nucleosynthesis is assumed to continue via various two-body reactions such as

$$\begin{aligned} {}^{3}\mathrm{He} + {}^{3}\mathrm{He} &\;\rightarrow\; {}^{4}\mathrm{He} + \mathrm{p} + \mathrm{p} \;, \\ {}^{3}\mathrm{He} + {}^{4}\mathrm{He} &\;\rightarrow\; {}^{7}\mathrm{Be} + \gamma \,. \end{aligned}$$

The Standard model is able to account for many (although not all) observable characteristics of the universe. Since its predictions are very sensitive to various parameters of the primordial plasma, the remaining discrepancies may be attributed either to wrong assumptions about these parameters or to the inadequacy of the model itself. It is therefore very important to scrutinize all the simplifications and approximations of the model before making conclusions. In the present work, we are concerned with

one of such simplifications, namely, the omission of triple collisions in the processes of deuteron formation.

Except for the so-called *pep* reaction (4.2), three-body collisions are omitted in the standard model. This is done on the grounds that they are less frequent. However, it is known that in three-body collisions there are more ways to satisfy the conservation laws (such as conservation of parity, angular momentum, and isospin) than in the two-body processes. As a result, three-body collisions are less restricted by various selection rules and therefore might make a noticeable contribution to the net production of certain nuclei when both two- and three-body initial states lead to the same final product. This kinematical difference between two- and three-body initial states means that some binary nuclear reactions suppressed by conservation laws can be eased due to the presence of a third particle.

In order to shed some light on the role played by triple collisions in the primordial formation of light nuclei, explicit calculations of three-body nuclear reactions are needed. Several articles on this matter were published in recent years [69, 70, 71, 72]. In the present work, we compare the rates of the three-body non-radiative process

$$\mathrm{e}^- + \mathrm{n} + \mathrm{p} \rightarrow \mathrm{d} + \mathrm{e}^- \tag{4.5}$$

and of the corresponding two-body reaction (4.3) which is included in the standard model of the Big Bang nucleosynthesis. The reaction (4.5) at low energies is of interest in nucleosynthesis in the stellar plasma as well.

By relating the abundances of light elements in the contemporary universe to the processes which took place during the first few minutes after the Big Bang, a theory of primordial nucleosynthesis enables astrophysicists to check various assumptions about

physical conditions prevailing at that time [73]. In particular, primordial production of deuterium is very sensitive to the baryon density and therefore predictions and measurements of deuterium abundance can be used to infer the density of baryons in the early universe. Besides this, the importance of studying primordial processes of deuterium formation follows from the fact that they represent the so-called "bottle neck" for synthesis of all other elements.

4.2 Reaction rate

According to the standard model, the primordial formation of nuclei started in $\sim 10^{-2}$ seconds after the Big Bang, with an average energy per particle of $\sim 10\,\mathrm{MeV}$ and the matter density $\sim 10^9\,\mathrm{g/cm^3}$. The Big Bang nucleosynthesis lasted about 100 seconds until the temperature dropped to $\sim 0.1\,\mathrm{MeV}$ and the density to $\sim 10\,\mathrm{g/cm^3}$. At the early stages, the primordial plasma is totally ionized, which means that the electrons are not associated to specific nuclei and can be considered as moving in continuum states, *i.e.* freely among the nuclei. Because of the high density, the average distances between the particles are small and the nuclei are closely surrounded by electrons. Hence, when two nucleons collide, there is always an electron nearby. The triple-collision processes (4.5) may therefore make a noticeable contribution to the formation of deuterons. In order to assess this contribution, we need to calculate the average reaction rate for all possible reactions (4.5) starting from different initial states characterized by different momenta of colliding particles.

Let $\Psi_{\mathbf{p}}$ be the wave function of the relative motion of the pn–pair with momentum $\mathbf{p}$

and let $\mathbf{k}$ be the momentum of the electron with respect to this pair. Let η represents a set of the discrete quantum numbers characterizing spin–isospin state of the three particles. Then, for the three–body collision process (4.5) with the initial and final energies E_i and E_f, the reaction rate per unit volume per second is defined by [74]

$$\mathcal{R}_3(\mathbf{p},\mathbf{k},\eta \longrightarrow \mathbf{k}',\eta') = \frac{1}{4\pi^2}\delta(E_f - E_i)\left|\langle \Psi_d,\mathbf{k}',\eta'|T|\Psi_{\mathbf{p}},\mathbf{k},\eta\rangle\right|^2 n_p n_n n_e \ , \tag{4.6}$$

where the states in the continuum are normalized as

$$\langle \Psi_{\mathbf{p}'},\mathbf{k}'|\Psi_{\mathbf{p}},\mathbf{k}\rangle = (2\pi)^6\delta(\mathbf{k}'-\mathbf{k})\delta(\mathbf{p}'-\mathbf{p}) \ ,$$

and T is the transition operator, Ψ_d is the wave function of deuteron, and n_p, n_n, and n_e represent the corresponding particle densities.

It is a standard assumption that in primordial plasma of the temperature θ the momenta $\mathbf{p}$ and $\mathbf{k}$ are distributed according to Maxwell's law [74]

$$\begin{aligned} N_{\mathbf{p}}(\theta) &= (2\pi\mu\kappa\theta)^{-3/2}\exp\left(-\frac{p^2}{2\mu\kappa\theta}\right) \ , \\ N_{\mathbf{k}}(\theta) &= (2\pi m\kappa\theta)^{-3/2}\exp\left(-\frac{k^2}{2m\kappa\theta}\right) \ , \end{aligned}$$

where $N_{\mathbf{p}}(\theta)$ and $N_{\mathbf{k}}(\theta)$ are the probability densities, μ is the proton–neutron reduced mass, m is the electron mass, and κ is the Boltzmann constant. We are concerned with the total rate of the transition from an initial state with any $(\mathbf{p},\mathbf{k},\eta)$ to a final state with all possible $\mathbf{k}',\eta'$. Thus the reaction rate (4.6) must be averaged over the initial quantum numbers $\mathbf{p},\mathbf{k},\eta$ and integrated over the final quantum numbers $\mathbf{k}',\eta'$. The averaging over $\mathbf{p}$ and $\mathbf{k}$ is achieved by summing-up the $\mathcal{R}_3$ for all possible values of these momenta with the weight factors $N_{\mathbf{p}}(\theta)$ and $N_{\mathbf{k}}(\theta)$ corresponding to their

probabilities, i.e.

$$\langle \mathcal{R}_3 \rangle_\theta = \frac{1}{M} \sum_{\eta\eta'} \int\int\int d\mathbf{p} d\mathbf{k} d\mathbf{k}' \, \mathcal{R}_3(\mathbf{p}, \mathbf{k}, \eta \longrightarrow \mathbf{k}', \eta') N_{\mathbf{p}}(\theta) N_{\mathbf{k}}(\theta) \ , \tag{4.7}$$

where M is the number of possible (initial) spin–isospin states.

Similarly to the two-body reaction theory where the average reaction rate $\langle \mathcal{R}_2 \rangle_\theta$ is written as a product of $\langle \sigma v \rangle_\theta$ (which is called the reaction rate per particle pair) and the particle densities [68] ,

$$\langle \mathcal{R}_2 \rangle_\theta = n_1 n_2 \langle \sigma v \rangle_\theta \ , \tag{4.8}$$

the three–body reaction rate $\langle \mathcal{R}_3 \rangle_\theta$ can also be factorized in the same manner,

$$\langle \mathcal{R}_3 \rangle_\theta = n_p n_n n_e \langle \Sigma \rangle_\theta \ , \tag{4.9}$$

where $\langle \Sigma \rangle_\theta$ is the three-particle reaction rate. Thus using Eqs. (4.6), (4.7) and (4.9), it follows that

$$\begin{aligned} \langle \Sigma \rangle_\theta \ &= \ \frac{1}{4\pi^2 M} \sum_{\eta\eta'} \int\int\int d\mathbf{p} d\mathbf{k} d\mathbf{k}' \, \delta(E_f - E_i) \times \\ &\quad \left| \langle \Psi_d, \mathbf{k}', \eta' | T | \Psi_{\mathbf{p}}, \mathbf{k}, \eta \rangle \right|^2 N_{\mathbf{p}}(\theta) N_{\mathbf{k}}(\theta) \ . \end{aligned} \tag{4.10}$$

4.3 Transition Amplitude

The motion of the nucleons is slow compared to that of the electron and thus can be treated adiabatically. Moreover, for the electron to participate in the three-body reaction (4.5), the two heavy particles (nucleons) must be close to each other when the electron arrives. Therefore the transition from the initial to the final state can be

viewed as a two-step process

$$|\mathbf{p},\mathbf{k}\rangle \stackrel{V_{pn}}{\Longrightarrow} |\Psi_{\mathbf{p}},\mathbf{k}\rangle \stackrel{V_{pe}}{\Longrightarrow} |\Psi_d,\mathbf{k}'\rangle \ ,$$

where V_{pn} and V_{pe} are the proton-neutron and proton-electron potentials. Therefore, instead of the transition

$$|\mathbf{p},\mathbf{k}\rangle \stackrel{V_{pn}+V_{pe}}{\Longrightarrow} |\Psi_d,\mathbf{k}'\rangle$$

caused by both V_{pn} and V_{pe}, in the adiabatic approximation, we may consider the transition

$$|\Psi_{\mathbf{p}},\mathbf{k}\rangle \stackrel{V_{pe}}{\Longrightarrow} |\Psi_d,\mathbf{k}'\rangle \ ,$$

where the interaction V_{pn} is already taken into account via using the scattering state $\Psi_{\mathbf{p}}$ instead of the plane wave $|\mathbf{p}\rangle$.

The adiabatic approximation also means that the transition operator T in Eq. (4.6) can be replaced by the fixed scattering T-matrix defined as

$$\tilde{T}(z) = V_{pe} + V_{pe}\frac{1}{z-h_0}\tilde{T}(z) \ , \tag{4.11}$$

where z is the total energy and h_0 is the kinetic energy operator associated with the momentum $\mathbf{k}$ of the electron. The Coulomb interaction between the proton and the electron can be treated perturbatively [70], which leads to the following series expansion for the transition operator

$$\tilde{T}(z) = V_{pe} + V_{pe}\frac{1}{z-h_0}V_{pe} + V_{pe}\frac{1}{z-h_0}V_{pe}\frac{1}{z-h_0}V_{pe} + \cdots \ . \tag{4.12}$$

For typical densities of the primordial plasma, the average potential energy $\langle V_{pe}\rangle$ $\sim 10\,\mathrm{eV}$ whereas the kinetic energy of the electrons is three orders of magnitude higher.

This means that the series (4.12) should converge very fast and we can thus retain only the Born term. In other words,

$$T \approx V_{pe} \ . \tag{4.13}$$

Therefore, instead of (4.10), we have

$$\begin{aligned} \langle \Sigma \rangle_\theta \ &\approx \ \frac{1}{4\pi^2 M} \sum_{\eta\eta'} \int\int\int d\mathbf{p} d\mathbf{k} d\mathbf{k}' \, \delta(E_f - E_i) \times \\ &\quad |\langle \Psi_d, \mathbf{k}', \eta' | V_{pe} | \Psi_\mathbf{p}, \mathbf{k}, \eta \rangle|^2 \, N_\mathbf{p}(\theta) N_\mathbf{k}(\theta) \ , \end{aligned} \tag{4.14}$$

which is the final formula used in our calculations. To calculate $\Psi_\mathbf{p}$ and Ψ_d entering this integral, we numerically solved the corresponding Schrödinger equation or equivalently the Faddeev equations, as is done in the present calculations, with the S-wave Malfliet-Tjon NN potential [41].

4.4 Numerical Calculations

Our starting point in the calculations is the computation of the reaction rates for the two- and three–body processes (4.3) and (4.5)

$$\langle \mathcal{R}_2 \rangle_\theta = n_p n_n \langle \sigma v \rangle_\theta \tag{4.15}$$

and

$$\langle \mathcal{R}_3 \rangle_\theta = n_p n_n n_e \langle \Sigma \rangle_\theta \tag{4.16}$$

in the same region of the plasma temperature. The radiative capture (4.3) has been studied for many decades and its theory can be found in a number of textbooks on nuclear physics. To calculate $\langle \sigma v \rangle_\theta$, we used the formulae given in [75].

Once $\langle \sigma v \rangle_\theta$ and $\langle \Sigma \rangle_\theta$ are calculated, the relative contribution of the triple non-radiative capture to the formation of deuterons can be estimated by calculating the ratio

$$\frac{\langle \mathcal{R}_3 \rangle_\theta}{\langle \mathcal{R}_2 \rangle_\theta} = \frac{\langle \Sigma \rangle_\theta}{\langle \sigma v \rangle_\theta} \, n_e \ , \tag{4.17}$$

in which the (poorly known) densities n_p and n_n are canceled out.

Eq. (4.17) shows that the contribution of the reaction (4.5) is proportional to the density of electrons. This density consists of two parts: The first being the density of "background" electrons (one per proton) and the second the density of electrons emerging from numerous electron–positron pairs continuously produced by strong electromagnetic radiation. The second part, corresponding to the "pair" electrons, is known to be dominant under the primordial nucleosynthesis conditions [76]. For this reason, we used the temperature dependent n_e [77]

$$n_e = \frac{1}{\pi^2} \left(\frac{mc}{\hbar} \right)^3 \left(\frac{\theta}{mc^2} \right) \, K_2(mc^2/\theta) \ , \tag{4.18}$$

which describes the density of the "pair" electrons. The presence of the modified Bessel function K_2 in the above equation, makes the density n_e extremely high at the very beginning of the nucleosynthesis, but exponentially vanishing when the plasma cools down. This means that the three–body processes (4.5) might give a noticeable contribution to the production of deuterons at least at high values of θ.

The results of our calculations for various plasma temperatures are given in Table 4.1. Unlike the cases considered in Refs. [70, 72, 73], it is found that the triple collisions (4.5) play a minor role as compared to that of binary reactions (4.3). This finding can be attributed mainly to the fact that the np system, in contrast to the other systems mentioned, has no Coulomb repulsion. Indeed, all the three-body reactions considered

earlier (such as $e^- + {}^3He + {}^4He \rightarrow e^- + {}^7Be$ in Ref. [73]) involve positively charged nuclei. The presence of the electron in a close vicinity of the nuclei reduces the repulsion between them and thus facilitates the fusion. This, of course, has no effect on the np system.

θ (keV)	θ (10^9 °K)	n_e (cm^{-3})	$\mathcal{R}_3/\mathcal{R}_2$
10	0.116	0.38×10^{06}	0.478×10^{-11}
20	0.232	0.13×10^{18}	0.171×10^{-09}
30	0.348	0.12×10^{22}	0.715×10^{-09}
40	0.464	0.13×10^{24}	0.166×10^{-08}
50	0.580	0.24×10^{25}	0.302×10^{-08}
60	0.696	0.17×10^{26}	0.482×10^{-08}
70	0.812	0.74×10^{26}	0.712×10^{-08}
80	0.928	0.23×10^{27}	0.999×10^{-08}
90	1.044	0.55×10^{27}	0.135×10^{-07}
100	1.160	0.11×10^{28}	0.177×10^{-07}
110	1.277	0.21×10^{28}	0.226×10^{-07}
120	1.393	0.35×10^{28}	0.282×10^{-07}
130	1.509	0.55×10^{28}	0.348×10^{-07}
140	1.625	0.81×10^{28}	0.421×10^{-07}
150	1.741	0.11×10^{29}	0.504×10^{-07}
160	1.857	0.16×10^{29}	0.596×10^{-07}
170	1.973	0.21×10^{29}	0.697×10^{-07}
180	2.089	0.26×10^{29}	0.808×10^{-07}
190	2.205	0.33×10^{29}	0.928×10^{-07}
200	2.321	0.41×10^{29}	0.106×10^{-06}
220	2.553	0.60×10^{29}	0.135×10^{-06}
240	2.785	0.83×10^{29}	0.167×10^{-06}
260	3.017	0.11×10^{30}	0.204×10^{-06}
280	3.249	0.14×10^{30}	0.244×10^{-06}

Table 4.1: Temperature dependence of ratio of the triple to binary reaction rates for the processes leading to formation of deuterons in primordial plasma.

Chapter 5

Applications II : Nuclear Systems

The present chapter's main objective is to perform calculations on three-body nuclear systems in configuration space in order to investigate in more detail the stability and performance of the algorithms described in this thesis. As testing cases we considered the triton and ^{6}Li systems. For the former system there are a lot of calculations to compare our results and check the suitability of our method with or without the inclusion of three-body forces. The ^{6}Li system on the other hand, because of the nature of the underlying two-body forces, requires in the traditional calculations a lot of partial waves to achieve convergence (especially when supersymmetric potentials are used), and therefore the check for stability of our algorithm in such an environment is crucial prior using the method in molecular cases which are much more sensitive to numerics and computationally more demanding.

5.1 Nuclear Potentials

In the case of triton, two nucleon-nucleon (NN) potentials were chosen for our test calculations. The first one is the Malfliet-Tjon potential [41, 42]

$$v^{(2\mathrm{B})}(r) = V_A \frac{e^{-\mu_A r}}{r} + V_R \frac{e^{-\mu_R r}}{r}\,, \tag{5.1}$$

where the first term is the long-range attraction and the second term represents the short-range repulsion. The second one is the Urbana v_{14} potential [43, 44]

$$v^{(2\mathrm{B})}(r_{\alpha\beta}) = \sum_{p=1,\cdots,14} \Big[v_\pi^p(r_{\alpha\beta}) + v_I^p(r_{\alpha\beta}) + v_S^p(r_{\alpha\beta}) \Big] O_{\alpha\beta}^p\,, \tag{5.2}$$

where v_π^p is the long-range one-pion exchange (OPE) potential, v_I^p the intermediate-range two-pion exchange potential, whilst v_S^p is the short-range part attributed to ω, ρ exchange, and where $O_{\alpha\beta}^p$ is a set of operators concerning spin, isospin, etc. In applications, however, the components corresponding to a particular isospin and spin (T, S) projections are used [78]. For example, the spin-singlet potential is written

$$v_{T,0}(r_{\alpha\beta}) = v_{\pi,T,0}(r_{\alpha\beta}) + \sum_{c,q} \Big[I_{T,0}^p T_\pi^2(r_{\alpha\beta}) + S_{T,0}^p W(r_{\alpha\beta}) \Big] O_{\alpha\beta}^p \tag{5.3}$$

whilst the spin-triplet one is

$$v_{T,1}(r_{\alpha\beta}) = v_{\pi,T,1}(r_{\alpha\beta}) + \sum_{p=c,t,b,q,bb} \Big[I_{T,1}^p T_\pi^2(r_{\alpha\beta}) + S_{T,1}^p W(r_{\alpha\beta}) \Big] O_{\alpha\beta}^p\,. \tag{5.4}$$

In Eqs. (5.3) and (5.4), T_π is the usual tensor cutoff function while I^p and S^p are parameters fixed via fitting the nucleon-nucleon data. For the three-body force we consider the Urbana type three-body interaction [79]

$$\mathcal{V}^{(3\mathrm{B})} = V_{\alpha\beta\gamma}^{2\pi} + V_{\alpha\beta\gamma}^{R}\,. \tag{5.5}$$

which is a sum of two-pion exchange term and a phenomenological short-range term. The explicit form employed in our work is that given in Ref. [80], i.e.

$$\mathcal{V}^{(3\mathrm{B})}(r_{\alpha\beta}, r_{\beta\gamma}, r_{\gamma\alpha}) = \sum_{\mathrm{cyc}} \Big[0.003 T_\pi^2(r_{\alpha\beta}) T_\pi^2(r_{\beta\gamma}) + 4.5 T_\pi(r_{\alpha\beta}) T_\pi(r_{\beta\gamma}) P_2(\cos\theta_\alpha) \Big] , \quad (5.6)$$

where

$$T_\pi(r) = \frac{\mathrm{e}^{-0.7r}}{r} \left(1 + \frac{3}{0.7r} + \frac{3}{(0.7r)^2} \right) \left(1 - \mathrm{e}^{-2r^2} \right)^2 , \quad (5.7)$$

$$P_2(x) = 0.5(3x^2 - 1) , \quad (5.8)$$

and the summation runs over the three cyclic permutations of particles α, β, and γ.

In the case of ^{6}Li, apart from the NN potential, one requires the α-nucleon (αN) interaction as input. From a computational point of view this means the coupled set of Faddeev equations to be solved read

$$\Big[\mathrm{H}_0 + v_{\alpha\mathrm{N}}^{(2\mathrm{B})} - E_{3\mathrm{B}} \Big] \Phi^{(1)} = -v_{\alpha\mathrm{N}}^{(2\mathrm{B})} \Big[\Phi^{(2)} - P_{\mathrm{NN}} \Phi^{(1)} \Big] \quad (5.9)$$

$$\Big[\mathrm{H}_0 + v_{\mathrm{NN}}^{(2\mathrm{B})} - E_{3\mathrm{B}} \Big] \Phi^{(2)} = -v_{\mathrm{NN}}^{(2\mathrm{B})} \Big[\Phi^{(1)} - P_{\mathrm{NN}} \Phi^{(2)} \Big] , \quad (5.10)$$

where P_{NN} is the permutation operator for the two nucleons, $v_{\mathrm{NN}}^{(2\mathrm{B})}$ and $v_{\alpha\mathrm{N}}^{(2\mathrm{B})}$ are the nucleon-nucleon and the effective nucleon-alpha interactions, respectively. The $\Phi^{(1)}$ is the Faddeev component corresponding to the (αN)-N configuration and $\Phi^{(2)}$ corresponds to the NN$-\alpha$ arrangement. The total wave function is then given by

$$\Psi_{3\mathrm{B}} = \Phi^{(2)} + (1 - P_{\mathrm{NN}}) \Phi^{(1)} \quad (5.11)$$

In applications, the effective αN interactions describing the spectrum of ^{6}Li are constructed using, for example, the microscopic theories such as the Resonating Group

Method (RGM) [81] or phenomenologically. Although the RGM interaction is well known and had been successfully used in $\alpha + n$ scattering [82], it has many drawbacks that makes it difficult to apply in few-cluster calculations. For example, it is nonlocal, energy-dependent, ℓ-dependent, contains the so-called Pauli forbidden bound states (PFS), and has a quite complicated form. On the other hand, phenomenological potentials are easy to use. However, they are generally quite deep and support also the unphysical PFS which must be removed before they are used in few-body calculations. There are several different ways to remove the PFS. First, one may construct *ab initio* a repulsive potential in the S-wave, so that no forbidden bound state is supported. Second, one can suppress the forbidden bound state by projecting it out. This can be handled equivalently via the use of the Marchenko inversion method to construct a local deep or shallow potential [83]. Another possibility is to apply supersymmetric transformation (SUSY) [84] to obtain from the local deep potential a shallow potential which produces the same phase shifts but has no PFS.

In this thesis we use the Malfliet-Tjon NN potential (5.1) and the phenomenological αN potentials Ref. [85]

$$V(r) = -V_0/[1 + \exp\{(r - R_0)/a\}]\,, \tag{5.12}$$

and of Ref. [86]

$$V(r) = V_0 \exp(-\beta r^2)\,. \tag{5.13}$$

The potential (5.12) is known to support a PFS. This we remove via the SUSY transformation yielding a potential having the $1/r^2$ behaviour at short distances. From a numerical point of view, as a result this behaviour, a large number of partial waves would be required in order to obtain convergence in binding energy calculations. For example, it was found that upto 75 channels were required to achieve convergence

in the binding energy for the isosinglet state configuration [87], with the number of channels doubling in the isotriplet configuration. In this work, however, we consider the calculations within the framework of the three-dimensional method as described in Chapter 3 and thus avoid the partial wave expansion. The only input into the model are the NN and the αN interactions, SUSY transformed or otherwise. Thus the ^{6}Li calculations will give a stringent test of our codes before they are used in molecular systems which are much more demanding.

Finally, we pass the following remarks in connection with the ^{6}Li nucleus. The existence of the tightly bound α-cluster makes the ^{6}Li nucleus a model few-body problem in the following sense. Instead of having to describe six independent nucleons, the presence of an α-cluster generates an effective three-body system composed of α-particle plus two nucleons, and thus the Faddeev techniques developed for the three-nucleon system can be applied [88].

5.2 Results for Triton

As a first test of our numerical method, and for comparison purposes, we calculate the binding energy of triton using the Malfliet-Tjon type potential (5.1). Specifically, we employ the spin-independent MT-V potential defined by parameters V_A = -570.3316 MeV fm, V_R = 1438.4812 MeV fm, μ_A = 1.55 fm^{-1} and μ_R = 3.11 fm^{-1}. We used $\hbar^2/M$ = 41.47 MeV fm^2, where M is the nucleon mass.

In order to optimize the accuracy of our method in calculating the binding energy, there are several parameters to vary. For example, the length parameter a_0, the grid

sizes (N_x, N_y, N_z), cutoff lengths ($x_{\max}$, $y_{\max}$), and the size of Krylov subspace. The a_0, which is the distance from the origin to the first nonzero value of the x-grid, is by far the important one, especially for molecular systems. A proper choice of a_0 is crucial for the following reason: A very small value of a_0 generates instabilities (due to the highly repulsive core of the underlying forces) that lead to the violation of the boundary conditions of the wave functions. In numerical terms the instabilities are due to the presence of large matrix elements in the system of equations. For this reason, the first step toward studying the accuracy of our method involves obtaining an optimal value for the length parameter a_0. This optimal value corresponds to the a_0 which yields a minimum binding energy for fixed, but not necessarily as yet optimal, grid sizes. To this end, we calculate the binding energy of triton (using the aforementioned Malfliet-Tjon type potential) as a function of a_0 for fixed N_x, N_y, and N_z. In Figure 5.1 we plot the results for the case $N_x = N_y = 20$, and $N_z = 2$. It is seen that the minimum energy occurs at about 0.042 fm, corresponding to E_{3B} = -7.0016372 MeV. To further check convergence, the binding energy calculations are repeated for $N_z = 3, 4, 5$. The results are given in Figure 5.2, with the converged binding energy of -7.7366192 MeV. It is clear from the figure that the binding energy is stable.

We already mentioned that for the aforementioned MT potential a plethora of results exist in the literature. This provides a benchmark upon which our results can be compared. To this end we compare our results with those obtained using (*i*). the integrodifferential equation approach (IDEA) [89, 90], and (*ii*). the Faddeev equation approach in the bipolar harmonics expansion [37]. These comparative results are shown in Table 5.1, where it can be seen that our results are in excellent agreement with others, especially where exact methods were employed.

Table 5.1: Triton binding energy (in MeV) for the MT-V potential. Here the results of our method are compared with those obtained by others.

This work	Ref. [89, 90]	Ref. [37]
-7.7366192	-7.73	-7.736600

Finally, we calculated the triton binding energy using both the two-body and three-body Urbana type interactions, given by Eqs. (5.2) – (5.8). Our results, given in Table 5.2, are compared with those of Ref. [80] where the same three-body force was used, albeit the two-body force employed was of the Malfliet-Tjon type with parameters adjusted to reproduce the binding energy of the deuteron. This explains the difference between the two results. We mention in passing that in [80] the Green's Function Monte Carlo method was employed. To end this section we pass the remark, mentioned elsewhere in this thesis, that calculations with three-body forces performed here are a test of the stability of our methods before they are employed in the more demanding molecular systems, where three-body forces are indispensable.

Table 5.2: Triton binding energy (in MeV) using both the two-body and three-body Urbana potentials. The results are compared with those of Ref. [80].

This work	Ref. [80]
-8.56250	-8.79

5.3 Results for ^{6}Li

As a second testing system in the application of our methods we consider the ^{6}Li nucleus, which is modeled as a three body system $^6\mathrm{Li} \rightarrow \alpha + \mathrm{N} + \mathrm{N}$. The ^{6}Li nucleus has many interesting characteristics. For example, it is one of the few stable odd-proton odd-neutron nuclei, it has a very large charge radius of about 2.56 fm compared to the value of 2.47 fm for the ^{12}C nucleus, with twice as many nucleons. In addition, the weak binding of ^{6}Li ground state with respect to the $\alpha + d$ break-up leads to a spatially extended configuration space, implying daunting numerical challenges in return.

From an experimental point of view, ^{6}Li can be used to extract information concerning momentum distributions of α+d and p+$(n\alpha)$, via the reactions $^6\mathrm{Li}(e, e'd)\alpha$, $^6\mathrm{Li}(p, 2p)\alpha$, $^6\mathrm{Li}(e, e'p)\alpha$ [91], for example. The information from these reactions is useful, first, in revealing the structure of nuclei, and second, in determining which α-nucleon models best describe the dynamics of the ^{6}Li when treated as a three-body system. Furthermore, ^{6}Li is of interest because it lends itself as a good candidate for a polarized target from which the polarized gluon distribution in a nucleon can be determined, as the following argument outlines. Conventional polarized proton targets are rare, and usually contain less than 20% polarization [92]. On the other hand, large targets containing ^{6}Li can be produced [93, 94], with as much as 50% polarization of the nucleons in ^{6}Li [87]. As a closing remark, we point out that polarized gluon distributions are needed to extract quark-antiquark distributions, which are of particular interest in medium- to high-energy studies [95, 96].

For the NN potentials we use the same interactions as for the triton. For the αN interaction we first employed the Satchler potential [85], characterized by the shape,

range, and depth parameters – a, R_0, V_0. In this work two sets of parameters were used. For the first set, hereunder referred as SET I, the parameters employed are those of Ref. [83], which are $V_0 = 41.8$ MeV, $R_0 = 2.376$ fm, $a = 0.25$ fm. The other set, which we shall refer to as SET II, uses the parameters given in [97], namely $V_0 = 43.0$ MeV, $R_0 = 2.00$ fm, and $a = 0.70$ fm. These potentials are quite deep and capable of sustaining unphysical bound states. Indeed it is known that the potential prescribed by SET I parameters supports a PFS at $\sim$ -9.0 MeV [83], whereas the potential defined by SET II parameterization supports a PFS with energy $\sim$ -9.8 MeV. As stated earlier these PFS must be removed before the potentials are used in few-body calculations. In this work the PFS are removed via the Supersymmetric transformation (SUSY) [83, 84], which yield shallow phase-equivalent local potentials (ELP), which do not support the PFS and have $1/r^2$ behaviour at short distances. The shapes of the two deep and shallow potentials are shown in Fig. 5.3 for SET II.

We also employed the Gaussian interaction of Sack-Biedenharnm-Breit [86], where the parameters are taken to be $V_0 = -47.32$ MeV, and $\beta = 0.189034$ fm^{-2} [97]. This potential is known to have an S-state PFS with energy $\sim$ -11.6 MeV. The SUSY-2 calculated binding energy results from all the potentials are given in Table 5.3. The results of Schellingerhout *et al.* [87], obtained by projecting out the PFS are also shown (for Woods-Saxon only) for comparison purposes. It is seen that our results are 15% deeper than those obtained via projection method. This can be attributed to the exact inclusion of all partial waves in our approach.

Table 5.3: The binding energy (in MeV) for the ^{6}Li nucleus calculated using SUSY αN potentials as input. These potentials are obtained from the transformation of the phenomenological potentials. The column labelled PFS gives the energies of the Pauli Forbidden States for the different models. For more details see text.

Model	PFS	Ref. [87]	SUSY
Ref. [83]	-9.80	-3.6	-4.07
Ref. [85]	-9.01	-3.7	-4.26
Ref. [97]	-11.6	–	-3.91

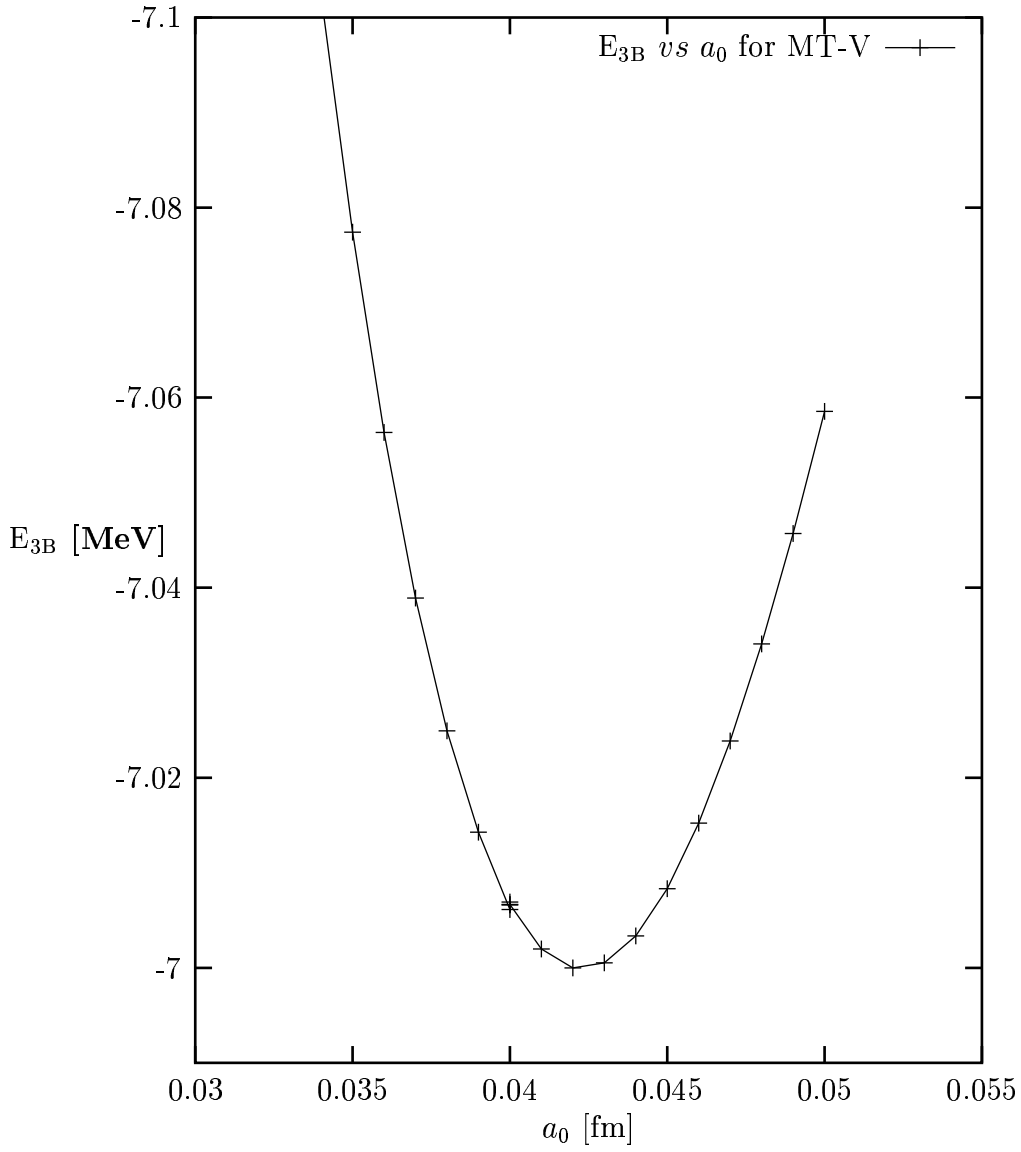

Figure 5.1: Triton binding energy (in MeV) as a function of a_0 for the MT-V potential.

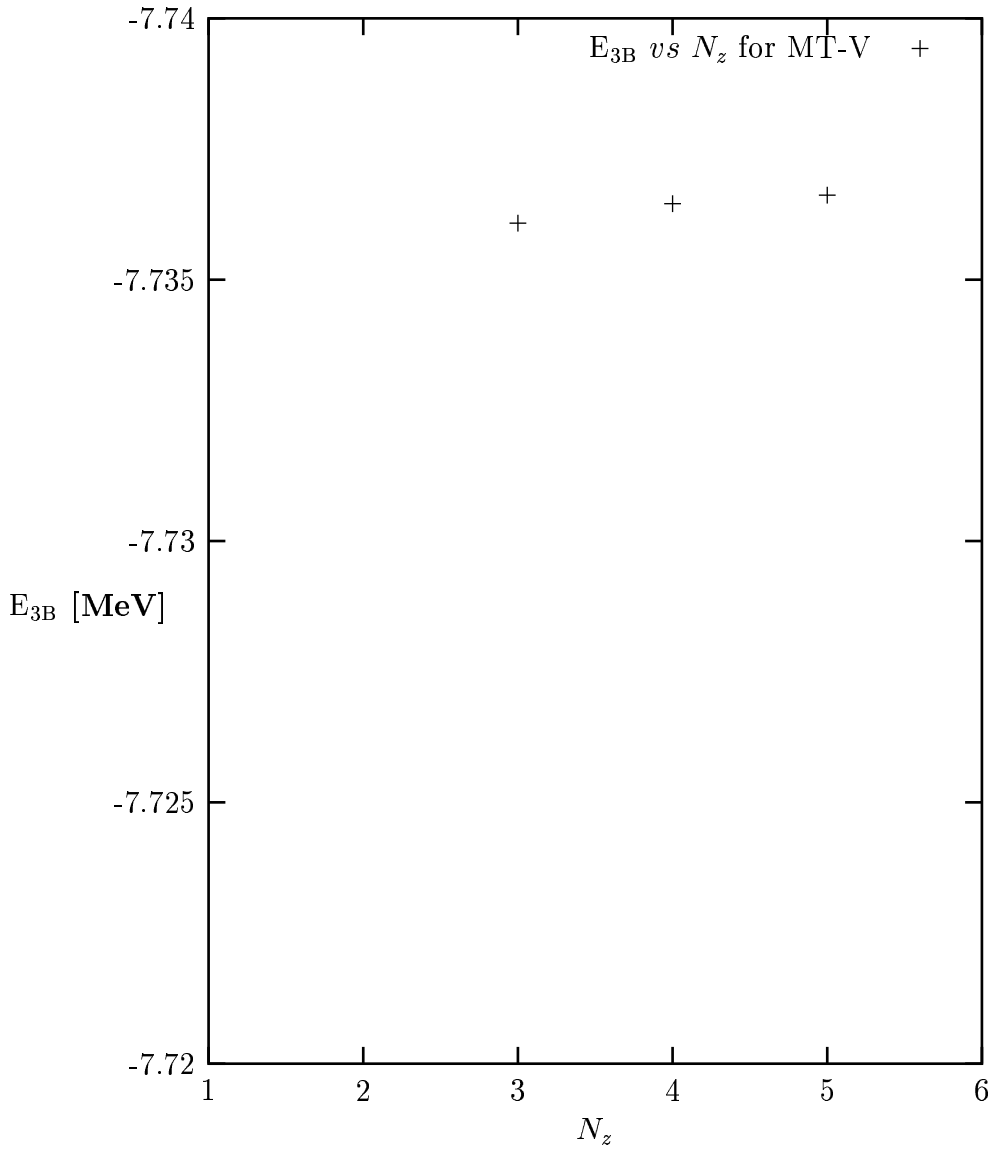

Figure 5.2: Triton binding energy (in MeV) as a function of $N_z = 3, 4, 5$ for the MT-V potential, at $a_0 = 0.042$ fm.

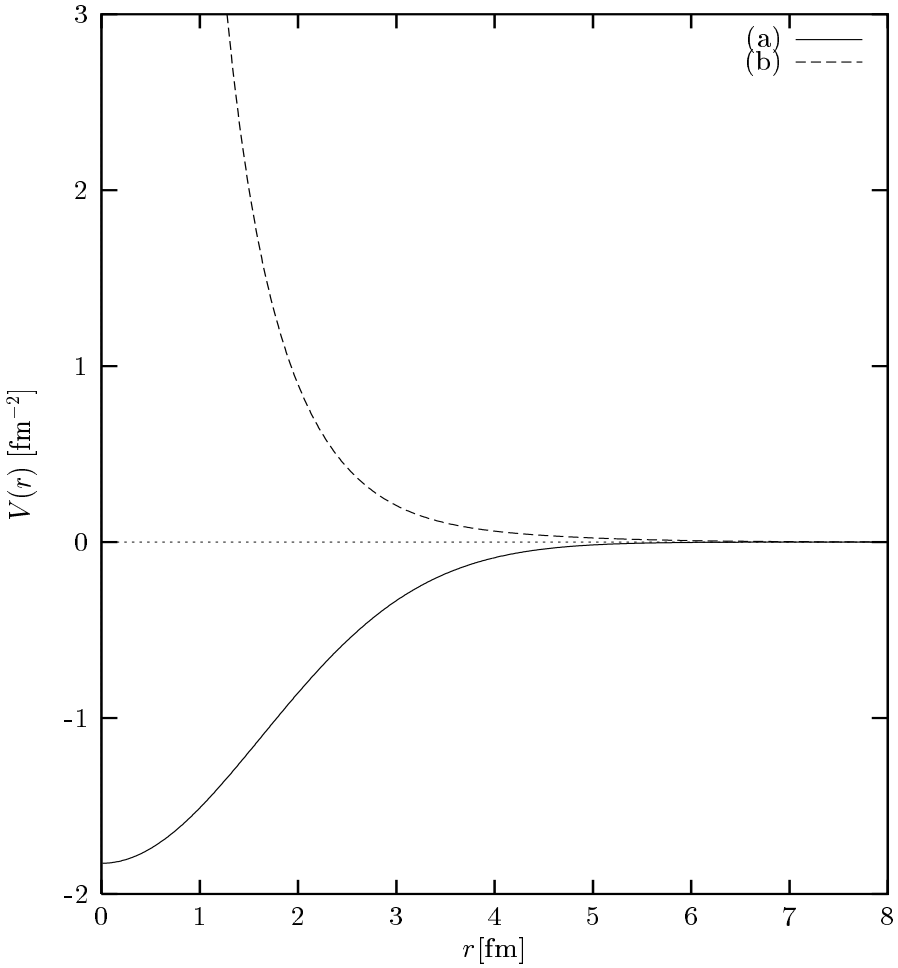

Figure 5.3: The Gaussian αN potentials of Ref. [97] and the SUSY partner. Graph (a) represents the Gaussian potential and (b) the SUSY partner.

Chapter 6

Applications III : Molecular Systems

In the preceding model calculations for triton and ^{6}Li, the suitability, and most importantly the stability of our three-dimensional methods has been established. In the present chapter we apply these methods to triatomic molecular systems. In particular we concentrate on the weakly-bounded trimers. As mentioned earlier, for these systems strong correlations exist as a consequence of interactions that are highly repulsive at short distances, and this necessitates the inclusion of a large number of partial waves in order to achieve convergence. This renders calculations cumbersome and unstable, and thus robust methods are required to obtain numerical solutions. We test the applicability of our method in addressing these difficulties by calculating vibrational spectra for the triatomic molecular systems. We first consider the ^{4}He trimer, which is known to be very weakly bounded, and then the Ozone molecule which has a plethora

of vibrational bound states, and in which the three-body interactions are expected to have significant contribution to the binding.

6.1 Molecular Hamiltonian

The Hamiltonian describing bound states of a polyatomic molecule contains in general, electronic, nuclear and spin coordinates. In order to treat the vibrational problem the various contributions to the Hamiltonian are separated. Because of the large difference between the mass of electrons and the masses of the nuclei, the separation between the electronic and nuclear motions is possible. Indeed, to a good approximation the electronic motions can be treated assuming fixed positions or very small amplitudes of the nuclei compared to the electronic motions. In this approximation, commonly known as the Born-Oppenheimer approximation [98], the Hamiltonian reads

$$\mathrm{H} = \mathrm{H}_e + \mathrm{H}_n \,,$$

where H_e is the electronic Hamiltonian, and H_n the contribution to the Hamiltonian due to the nuclei. Thus the wave function of the system is a product of the nuclear wave function ψ_n and the electronic wave function ψ_e. In this way, the electronic wave function is an eigenfunction of H_e, i.e.

$$\mathrm{H}_e\psi_e = E_e\psi_e \,, \tag{6.1}$$

for a fixed nuclear configuration, while the nuclear wave function satisfies

$$(\mathrm{H}_n + E_e)\psi_n = E\psi_n \,. \tag{6.2}$$

Furthermore, the nuclear motion can be separated into vibrational and rotational motions. Within the framework of the Born-Oppenheimer approximation one writes

$$\mathrm{H}_n = \mathrm{H}_v + \mathrm{H}_r \tag{6.3}$$

where H_r is the rotational Hamiltonian and H_v is the vibrational Hamiltonian satisfying the equation

$$\mathrm{H}_v \psi_v = E_v \psi_v \,. \tag{6.4}$$

For identical atoms H_v ($\hbar^2/2m = 1$) is given by

$$\mathrm{H}_v = -\frac{\partial^2}{\partial x^2} - \frac{\partial^2}{\partial y^2} - \left(\frac{1}{x^2} + \frac{1}{y^2}\right) \frac{\partial}{\partial z}(1 - z^2)\frac{\partial}{\partial z} + V(x, y, z)\,, \tag{6.5}$$

$$= \mathrm{H}_0 + V(x, y, z) \tag{6.6}$$

where $z = \cos\theta$, and θ the angle between the Jacobi vectors $\mathbf{x}$ and $\mathbf{y}$. The free Hamiltonian H_0 is identical to (2.17) while V is the sum of two- and three-body forces. Hence, the methods of Chapter 2 can be applied to study the vibrational dynamics of triatomic molecules.

6.2 Helium Trimer

Of the many studies involving small clusters of atoms, the ^{4}He trimer has received a considerably more attention, both experimentally [99, 100, 101, 102] and theoretically [103, 104, 105, 106, 107, 108], to give but a few references. There are several reasons for this. For example, understanding properties of the helium trimer is a doorstep towards understanding the properties of helium liquid drops, superfluidity in helium films, and

Bose-Einstein condensation. On the other hand, since the binding energy of the ^{4}He dimer is extremely small, the helium trimer lends itself as a natural candidate where the Efimov effect [109] can be observed. From a practical point of view, the problem of three helium atoms is an ideal three-boson system since ^{4}He atoms are neutral atoms and one does not have complications due to spin, isospin, or Coulomb interaction, to worry about.

Most theoretical investigations on helium clusters are based on variational methods [106], hyperspherical harmonic expansions [107, 108], Faddeev equation based on partial wave expansion [103, 104, 105], just to mention a few recent investigations. Recently binding energy results were obtained using the three-dimensional Faddeev differential equations in the total-angular-momentum representation [110]. We must mention here that from our experience in the triton case, the two methods (viz. finite difference method and total-angular-momentum representation method) are similar and gave to all practical purposes the same results. However, we find the total-angular-momentum method more suitable. Thus from now on we will use the total-angular-momentum representation technique.

The reason for using the helium trimer as our first application of our method is that there is a vast amount of literature work on helium clusters and thus comparison is easy. In addition, the helium trimer is an ideal starting point because the contribution of the three-body forces to the binding energy is known to be negligible, of the order of 1%. Neglecting three-body forces renders easy calculations by avoiding the complexities and ambiguities associated with the presence of these forces.

6.2.1 He-He Interactions

In spite of simplicities mentioned in the previous section, the numerical handling of $^4He_3$ is quite formidable. The calculation of its binding energy is therefore a good testing ground for investigating stability and reliability of any numerical method in molecular calculations. The difficulties are due to the weak nature of the attraction in the interaction as compared to the, practically, hard repulsive core.

One of the earliest work concerning the microscopic study of the ground state properties of composites made of helium atoms used the Lennard-Jones type He-He interaction [111], which is a sum of only one attractive and repulsive terms. However, as it is well known there is no theoretical justification for the repulsive R^{-12} asymptotic dependence. It was used as a matter of convenience to counteract the attractive part. Another widely used interaction is the Morse potential, which also suffers from the drawback that it does not reproduce the asymptotics correctly. In recent years realistic He-He interactions were developed. We mention, for example, the HFD-B [112], LM2M2 [113] potentials of Aziz and co-workers, and the so-called TTY potential [114] due to Tang, Toennies and Yiu. For completeness the analytic forms of these potentials are given in the Appendix A.1.

6.2.2 Results

For calculations of the binding energies we employed the above mentioned HFD-B, LM2M2 and TTY realistic potentials. We used $\hbar^2/M = 12.12$ K Å^2. As described in the previous chapter, the crucial steps in the application of our numerical method lies in

determining the optimal controlling parameters a_0 and cutoff radii $x_{\max}$, $y_{\max}$. For $^4He_3$ system very large domains Ω_x, Ω_y in the configuration spaces of the coordinates x and y are necessary. This is a consequence of the low binding energy of the corresponding helium dimer $^4He_2$. Typical grid sizes are given in Table 6.1 where the calculated ground state binding energies are shown with optimala_0.

Table 6.1: The binding energies (in K) of the ground state $^4He_3$ for the potentials: HFD-B [112], LM2M2 [113], and TTY [114]. The top part of the table gives results obtained in this work as a function of the grid sizes. The bottom part of the table give results obtained by others using different methods.

N_x	N_y	N_z	HFD-B	LM2M2	TTY
50	50	3	-0.1385316	-0.1218115	-0.1209365
100	100	3	-0.1350168	-0.1269019	-0.1268981
150	150	3	-0.1324774	-0.12641587	-0.12642109
200	200	3	-0.1321926	-0.12641020	-0.12641001
Ref. [107]			–	-0.1061	–
Ref. [108]			–	-0.1252	–
Ref. [103]			-0.131	–	–
Ref. [110]			-0.13298	-0.1264	-0.1264

For the HFD-B potential, our results are compared with those of Refs. [103] and [110], both of which use the differential Faddeev equations approach. More specifically, the approach in [110] is similar to the one employed in this work, while in [103] the boundary condition method [115, 116] was employed. In [107], and [108] the adiabatic hyperspherical harmonics expansion methods were used.

It is seen that the exact inclusion of all partial waves give results in good agreement and as expected the binding energies are slightly deeper that those of other methods based on partial wave expansion. For example, the results of Motovilov *et al.* [103] (where only the $\ell = 0.2$ partial waves were include) also show a slight difference.

6.3 Ozone Molecule

The Ozone molecule is a very important gas in the upper atmosphere, and there has been a large amount of research in studying its structure and spectra, both experimentally [117, 118, 119, 120] and theoretically [121, 122, 123, 124]. It differs from the $^4He_3$ in a number of aspects. From a numerical point of view, the computation of the vibrational spectrum for Ozone is quite demanding, mainly for two reasons. First, it has many vibrational levels. In this respect, the calculation of the vibrational spectrum of the ozone must proceed, in approaches where adiabatic approximations are used, with the use of different potential energy surfaces for different electronic configurations. Second, the many vibrational levels lie very close to one another, a task that leads to convergence and efficiency problems. To avoid these difficulties refined numerical methods and avoidance of partial wave decomposition are needed. We handle the numerous states via the use of a global minimization method.

6.3.1 Interactions

Unlike the ^{4}He trimer case, where the neglect of three-body forces in calculating binding energy is justified, investigating the dynamics of the Ozone molecule requires the use of both two- and three-body interactions. The latter arise from the same sources as the two-body forces, i.e. polarization, dispersion, and exchange repulsions, etc. In this work only long-range dispersion-type three-body interactions of the Axilrod-Teller-Muto form [50, 51] are considered, mainly for two reasons. First, they are well known compared to the exchange interactions, for example. Second, it is known that when used in conjunction with the so-called "good" pair potential they lead to accurate description of experiments on dense rare gases in liquid and solid phases [125]. For completeness, we mention that by a good pair potential we mean a potential that should reproduce, at best, the purely pair properties such as viscosity and dimer spectroscopy. One such good two-body interaction, which we employ in this work, is that by Varandas *et. al.* [123]

$$v_i^{(2B)}(r_i) = A\Big[1 + a_0(r_i - R_0)\exp[-a_0(r_i - R_0)]\Big], \quad i = \alpha, \beta, \gamma\,; \tag{6.7}$$

where the parameters A, a_0 and R_0 are given in Table 6.2.

Table 6.2: Parameters for the two-body potential for Ozone.

Parameter	Value
A	- 5.21296 MeV
a_0	3.75374 Å^{-1}
R_0	1.2074 Å

The form of the Axilrod-Teller three-body interaction used in this work is given in the Appendix.

6.3.2 Minimization

The problem of calculating the binding energies is equivalent to finding the discrete spectrum of the operator

$$\hat{\mathcal{F}} = -(\hat{\mathrm{H}}_1 - E_{3\mathrm{B}}\hat{I})^{-1}\hat{\mathrm{H}}_2\,, \tag{6.8}$$

where $\hat{\mathrm{H}}_1$ and $\hat{\mathrm{H}}_2$ are as defined in Eq. 3.7. In the presence of many excited states $(E_\lambda, \lambda = 1, 2, 3\cdots)$ the corresponding eigenvalue equation, $\hat{\mathcal{F}}\Phi = \Lambda\Phi$, can be transformed into a minimization problem for the functional, given by Eq. 3.29, that is

$$I(E_\lambda) = \frac{\sum_i [\mathcal{F}\Psi_\lambda(x_i, y_i, z_i) - \Lambda_\lambda(E_\lambda)\Psi_\lambda(x_i, y_i, z_i)]^2}{\sum_i [\Psi_\lambda(x_i, y_i, z_i)]^2}\,, \tag{6.9}$$

where, as mentioned, Ψ_λ is the eigenfunction defined on the collocation points (x_i, y_i, z_i). As before, the eigenvalue $\Lambda_\lambda = 1$ corresponds to a physical solution for the binding energy E_λ, and is obtained using global minimization methods. For more details concerning the methods employed here we refer to Refs. [59, 60, 65, 126, 127].

In practice, our implementation of the above method proceed as follows: The Arnoldi method is used to obtain trial eigensolutions for a given energy range $E_0 \leq E_\lambda \leq E_1$ in the manner described in Chapter 3. Provided the chosen range bounds is valid, as tested

by the Arnoldi method, an interface routine named OPTIMA is called to implement a multistart approach for the global optimization. In other words, a number of points are generated, and from each one a local search is started. Thus, within a specific energy range the method provides all binding energies, corresponding to the specific grids used, and therefore the convergence of results can be easily checked.

6.3.3 Results

The purpose of our calculations is twofold. First, to test the accuracy of our algorithms in the presence of both two- and three-body forces. Second, since the ozone molecule is known to have a plethora of states, the determination of the the low-lying spectrum of the ozone molecule is a test of how far our methods (Arnoldi + global minimization) handle such systems. The two- and three-body forces used in the present work are those of Varandas *et al.* [123], whose analytic forms are given in the Appendix. Using the above interactions we obtain the binding energies for the first five states' which are shown in Table 6.3. Also in Table 6.4, results obtained using the density functional theory method are shown for comparison.

Table 6.3: The binding energies (in eV) of the low-lying states ($n = 0, 1, 2, 3, 4$) of the Ozone molecule. The column labeled Δ indicates the difference in binding energy calculated with two-body forces (2BF) only, and with both two- and three-body forces (2BF+3BF).

State, n	2BF	(2BF + 3BF)	Δ
0	-10.051	-13.423	3.372
1	-9.9014	-12.095	2.194
2	-8.5100	-11.432	2.922
3	-8.0902	-11.286	3.196
4	-8.0012	-10.523	2.522

Table 6.4: Comparisons of the binding energies (in eV) of the low-lying states of Ozone obtained with others.

State, n	2BF	(2BF + 3BF)	Ref. [128]
0	-10.051	-13.423	-9.91
1	-9.9014	-12.095	-9.00
2	-8.5100	-11.432	-8.49
3	-8.0902	-11.286	-8.20
4	-8.0012	-10.523	–

Chapter 7

Discussion and Conclusions

Dynamics of few-body systems can be investigated using integral equations in momentum space or differential equations in configuration space. In the present thesis we used configuration space differential equations to investigate certain three-body bound state and momentum space equations to calculate reaction rates for triple collision processes.

Within the momentum space approach we studied the role played by triple collision reactions, which are usually neglected in the standard model of primordial nucleosynthesis, in the formation of light elements. More specifically we studied the non-radiative process $e^- + n + p \to d + e^-$, calculating its reaction rate at energies of interest in nucleosynthesis. The main finding of our investigations are that the aforementioned triple collisions play a minor role compared to its binary reaction counterpart $n + p \to d + \gamma$. This conclusion is attributed to the following fact: The presence of the electron in close vicinity of the nucleons reduces the repulsion between them and thus facilitates

the fusion, albeit the influence is small.

On the other hand, within the configuration space approach, where our main focus is, we investigated the possibility of solving directly three-dimensional equations, obtained within the Faddeev theory, without resorting to an explicit partial wave decomposition. Although the latter reduces the Faddeev equations into a coupled two-variable integrodifferential equations, they are not always advantageous, especially when the underlying two-body interactions give rise to strong two-body correlations in which a large number of partial waves are required to achieve convergence. As the number of coupled channel equations increases, the solution of the seemingly simpler two-variable equations become cumbersome and unstable. These problems are especially manifested in molecular systems where the interatomic van der Waal interactions have a practically repulsive hard-core, requiring the inclusion of large partial waves in the subsystems involved.

Our first main concern was, therefore, to develop a numerical method to solve the configuration space Faddeev equations in the total-angular-momentum representation and test the method in a wide range of three-body bound systems. These include

- nuclear three-body systems, and
- triatomic molecular systems.

Insofar as molecular systems are concerned our focus was the calculation of the vibrational spectra of the weakly bounded molecular systems, which is generally a formidable task to implement.

Our second concern was to address the question of how well does the Faddeev-type

equations describe the dynamics of the weakly-bounded molecular systems with pairwise interactions, and the role played by three-body forces in these systems which is expected to be more important than in nuclear systems. Our main findings can be summarized as follows:

A. Numerical Methods

1. From a practical point of view, the huge matrices involved in the eigenvalue problem associated with the three-dimensional Faddeev equations are handled using the tensor-trick technique. The matrices are obtained using the triquintic Hermite splines which require three collocation points, which were chosen using Gaussian quadratures. This was found to be decisive compared to two points required by the Hermite cubic splines. In order to address the convergence difficulties, which always arise in situations where huge spaces are involved, as in the case of weakly bounded systems, we supplemented the restarted Arnoldi method by the Chebyshev polynomial acceleration technique. Furthermore, the formidable task of handling systems with plethora of states, is addressed by combining the aforementioned methods with the global minimization strategy.

2. Concerning the discretization of the spaces, two remarks may be passed: First, the choice of the $x-$grid is very crucial since it must reproduce the binding energy of the two-body subsystem. Second, we found that distributing the $x-$ and $y-$grid knots quadratically improves efficiency. The crucial point here, of course,

is that the grids should be dense in regions where the potentials are the strongest.

3. The use of triquintic Hermite splines in conjunction with the Arnoldi method and the tensor-trick gave stable results that are comparable to those obtained by other methods, and therefore the handling of three-dimensional bound state without partial wave decomposition is not only possible but desirable, especially for molecular systems.

B. Nuclear systems

1. We employed our numerical methods to solve the three-nucleon problem (as a bosonic system) with semi-realistic nucleon-nucleon Malfliet-Tjon V interaction, as well as the two- and three-body potentials of the Urbana type. The results obtained in both cases are in agreement with those obtained via other methods, for example, hyperspherical harmonics expansion approach, partial wave decomposition of the Faddeev equations, and Green Function Monte Carlo Method. Moreover, the numerical implementation of three-body forces in the Faddeev equations presented no problem. Therefore our method can be safely used for any three-nucleon calculations in configuration spaces.

2. As a three-cluster nuclear system we consider the ^{6}Li, which can be modeled as a $n + p + \alpha$ system, in an isospin-invariant formalism. One of the main challenges here is the removal of the unphysical Pauli Forbidden States (PFS) associated

with the $\alpha + \mathrm{N}$ potentials. There are various ways in which this can be handled. One way is to use the Supersymmetric Transformations (SUSY) [84, 83]. As is well known, this approach yields unique, local, and shallow singular potentials (behaving as $1/r^2$ at short distances) which can be used for three-body bound state calculations. We mention that the resulting highly repulsive potential would require the use of many partial waves in calculations that employ partial wave decomposition approach. Since in this work the equations are solved directly without explicit partial wave decomposition the question of the number of partial waves to be included is avoided.

3. Despite the $1/r^2$ behaviour of the SUSY-2 potentials the results are stable, indicating once more that the solution of the three-dimensional equations is reliable.

C. Molecular systems

1. The calculation of the many excited vibrational states present in the Ozone spectrum, is always a challenge irrespective of the method employed. These states lie very close to one another and therefore lead to slow convergence and stability problems. In this thesis, we combine the Arnoldi method together with a global minimization strategy to overcome this. The minimization strategies employed proved to be very useful and provides all binding energies within a specific range and accuracy.

2. Another challenge here is the inclusion of the three-body force in the Faddeev equations. The inclusion of three-body forces leads to even more formidable numerical challenges. However, the use of Arnoldi method in conjunction with other techniques, such as the tensor-trick method, polynomial acceleration of the solution, made the problem manageable.

3. The inclusion of the three-body forces yield additional binding which depends on the system considered. For the ^{4}He the additional binding was rather small. However, for the Ozone molecule a considerable additional binding (of the order of 20%) was realized. Thus, the inclusion of three-body forces, whenever calculations for triatomic molecular systems spectra are required, is in general warranted.

4. Finally, we pass a general comment on the nature of interatomic interactions for polyatomic molecules. For these systems different electronic states are possible, and therefore one requires many potential surfaces. However, in our approach a single potential function is used in calculations.

D. Future Research

1. We mentioned elsewhere in this thesis that the use of three-body forces in the investigation of three-body dynamics, especially in molecular cases, is in general warranted. However, in cases where the parameters of the three-body force are not known, say from experiment, one need a reliable theoretical way to determine them. Through the use of optimization techniques within the MERLIN packages,

this work paves the way to a secure method for determining such parameters for a three-body potential under the requirement that a combination of a realistic two-body force together with the three-body force will reproduce binding energies of a number of low-lying states.

2. In all cases treated in this work, the methods employed proved accurate and reliable. Hence their extension to scattering problems, as well as other bound state problems of higher complexity or dimensionality, is warranted. We mention in passing, however, that in the scattering case for molecular systems one has to be extremely careful since the underlying two-body interactions might violate the Levinson theorem for the corresponding phase shifts, due to their hard core behaviour.

3. The method can also be employed in studies involving recombination processes at ultra-low energies, photochemistry processes, etc.

4. The behaviour of trimers under certain thermodynamical conditions, especially those close to phase transitions are of extreme interest in understanding the influence of two- and three-body forces on gas-liquid coexistence of trimers. The methods described in this thesis can be used to address these questions.

Appendix A

Molecular Interactions

This appendix contains explicit analytic expressions for molecular interactions employed in this work.

A.1 He-He Interactions

Three different types of two-body interactions were used in the ^{4}He trimer calculations. These are: (*i*). the Hatree-Fock type potential [112], (*ii*). the so-called LM2M2 potential of Aziz & coworkers [113], and (*iii*). the aptly named TTY potential of Tang, Toennies and Yang [114]. Their explicit expressions are

$$V_{\rm HFD-B}(r) = \varepsilon V_0(x)\,, \tag{A.1}$$

$$V_{\rm LM2M2}(r) = \varepsilon\Big[V_0(x) + V_{\rm add}(x)\Big]\,, \tag{A.2}$$

$$V_{\rm TTY}(r) \;=\; A\Big[V_{\rm ex}(r)+V_{\rm disp}(r)\Big]\,, \tag{A.3}$$

where

$$\begin{aligned}
V_0(x) &= A\exp(-\alpha x+\beta x^2)-\left(\frac{C_6}{x^6}+\frac{C_8}{x^8}+\frac{C_{10}}{x^{10}}\right)F(x)\\
V_{\rm add}(x) &= \begin{cases} A_a\Big[\sin\left(\frac{2\pi(x-x_1)}{x_2-x_1}-\frac{\pi}{2}\right)+1\Big]\,, & x_1\le x\le x_2\,,\\ 0\,, & x\notin[x_1,x_2]\,. \end{cases}\\
V_{\rm ex}(r) &= Dr^{(7/2\beta-1)}\exp(-2\beta r)\,,\\
V_{\rm disp}(r) &= -\sum_{n=3}^{N}C_{2n}\frac{f_{2n}(r)}{x^{2n}}\,.
\end{aligned}$$

and $x=r/r_m$. The functions $F(x)$ and f_{2n} are defined by

$$\begin{aligned}
F(x) &= \begin{cases} \exp(-(D/x-1)^2)\,, & x\le D\,,\\ 1\,, & x>D\,, \end{cases}\\
f_{2n}(r) &= 1-\exp(-br)\sum_{k=0}^{2n}\frac{(br)^k}{k!}
\end{aligned}$$

where $b(r)=2\beta-(7/2\beta-1)r^{-1}$. The various parameters for the above potentials are given in Tables A.1.

Table A.1: Parameters for the He-He potentials.

Parameter	HFD-B	LM2M2	TTY
ε (K)	10.948	10.97	–
r_m (Å)	2.963	2.9695	–
A	184431.01	189635.353	315766.2067
α	10.43329537	10.70203539	–
β	-2.27965105	-1.90740649	1.3443
C_6	1.36745214	1.34687065	1.461
C_8	0.42123807	0.41308398	14.11
C_{10}	0.17473318	0.17060159	183.5
D	1.4826	1.4088	7.449
A_a	–	0.0026	–
x_1	–	1.003535940	–
x_2	–	1.454790369	–

A.2 Ozone Three-body Interactions

Using perturbation theory it can be shown that the long-range triple-dipole three-body interaction is given by a simple analytical expression of the form [50, 51]

$$\mathcal{V}^{(3B)}(r_\alpha, r_\beta, r_\gamma) = C\Big[\frac{1 + 3\cos\theta_\alpha \cos\theta_\beta \cos\theta_\gamma}{(r_\alpha r_\beta r_\gamma)^3}\Big], \tag{A.4}$$

where C is the constant characteristic of a system, and the coordinates r_i, θ_i, $(i = \alpha, \beta, \gamma)$ are, respectively, the internuclear distances, and internal angles of the triangle formed by the three atoms making up the system as shown in Figure A.1.

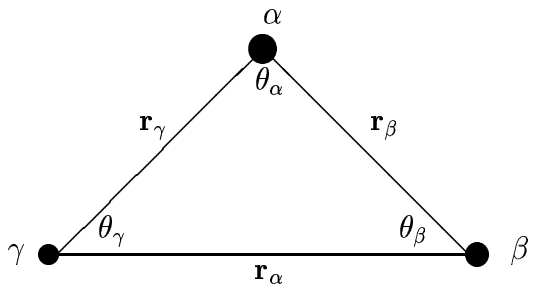

Figure A.1: The coordinates for a triatomic molecule.

Also three-body Ozone potential may be given in terms of symmetry-adapted coordinates Q's. In terms of these coordinates, the ground state potential reads [123]

$$\mathcal{V}^{(3B)}(r_\alpha, r_\beta, r_\gamma) = \Big[P(r_\alpha, r_\beta, r_\gamma) + G(r_\alpha, r_\beta, r_\gamma)\Big]\Big[1 - \tanh\gamma_0 Q_1/2\Big]; \tag{A.5}$$

$$\begin{aligned} \text{where} \quad P(r_\alpha, r_\beta, r_\gamma) \;=\; & a_1 + a_2 Q_1 + a_3 Q_1^2 + a_4(Q_2^2 + Q_3^2) + a_5 Q_1(Q_2^2 + Q_3^2) \\ & + a_6(Q_3^3 - 3Q_2^2 Q_3) + \; a_7(Q_2^2 + Q_3^2)^2\,, \end{aligned} \tag{A.6}$$

$$G(r_\alpha, r_\beta, r_\gamma) \;=\; (b_1 + b_2)\Big[b_3 + \sum_{i=\alpha,\beta,\gamma} (r_i^2 - r_j^2 - r_k^2)/2r_j r_k\Big]^5 \exp(-b_4(Q_2^2 + Q_3^2)\,. \tag{A.7}$$

The various parameters for this potentials are given in Table A.2.

Table A.2: Parameters for the ozone potential. Distances in Å.

Parameter	Value
$\tilde{R}_0$	1.5698
γ_0	4.4
a_1	7.9920
a_2	6.1872
a_3	12.4339
a_4	-15.1314
a_5	-3.2418
a_6	2.6323
a_7	12.4195
b_1	3941.4453
b_2	3909.5196
b_3	1.2527
b_4	0.8

Appendix B

Coordinate Transformations

The formalism in this work was presented in terms of the Jacobi coordinates described from Chapter 2. However, as seen above, the potentials are not always given in these coordinates. For example, the triple-dipole potential is prescribed in coordinates of Figure A.1 and not the Jacobi coordinates of Figure 2.1. The two coordinates systems are related via the following relationship

$$r_1 = x\,, \tag{B.1}$$

$$r_2^2 = y^2 - \frac{2m_A}{m_A+m_B}xy\cos\theta + \left(\frac{m_A}{m_A+m_B}\right)^2 x^2\,, \tag{B.2}$$

$$r_3^2 = y^2 + \frac{2m_B}{m_A+m_B}xy\cos\theta + \left(\frac{m_B}{m_A+m_B}\right)^2 x^2\,. \tag{B.3}$$

On the other hand the transformation between the symmetric coordinates Q_i's and the

r_i's is defined by

$$\begin{pmatrix} Q_1 \\ Q_2 \\ Q_3 \end{pmatrix} = \begin{pmatrix} \frac{1}{\sqrt{3}} & \frac{1}{\sqrt{3}} & \frac{1}{\sqrt{3}} \\ 0 & \frac{1}{\sqrt{2}} & -\frac{1}{\sqrt{2}} \\ \frac{\sqrt{2}}{\sqrt{3}} & -\frac{1}{\sqrt{6}} & -\frac{1}{\sqrt{6}} \end{pmatrix} \begin{pmatrix} r_1 - \tilde{R}_0 \\ r_2 - \tilde{R}_0 \\ r_3 - \tilde{R}_0 \end{pmatrix}, \tag{B.4}$$

where $\tilde{R}_0$ is the equilibrium position of system, and the r_i's are given by B.3.

Bibliography

[1] H. A. Bethe, R. F. Bacher, Rev. Mod. Phys. **8**, 82 (1936).

[2] B. H. Flower, F. Mandl, Proc. R. Soc. London, **A206**, 131 (1950).

[3] L. D. Faddeev, Sov. Phys. JETP **2**, 1014 (1961); see also: L. D. Faddeev, *Mathematical Aspects of the Three Body Problem in Quantum Scattering Theory* (Israel Program for Scientific Translation, Jerusalem, 1965).

[4] P. Grassberger, W. Sandhas, Nucl. Phys. **B2**, 181 (1967).

[5] E. O. Alt, P. Grassberger, W. Sandhas, Nucl. Phys. **1**, 167 (1967).

[6] W. Sandhas, Acta Physica Austriaca, Suppl. **IX**, 57 (1972).

[7] H. P. Noyes, H. Fiedeldey, in *Three-particle scattering in Quantum Mechanics, Proceedings of the Texas A & M Conference*, Eds. Gillespie J. and Nuttall J. (Benjamin Inc, 1968).

[8] H. P. Noyes, Phys. Rev. Lett. **23**, 1201 (1969).

[9] H. P. Noyes, in *Three-Body Problems in Nuclear and Particle Physics*, *Proceedings of the 1st Int. Conf. on the Three-Body Problem in Nuclear and Particle Physics*, Eds. McKee J. S. C. and Rolph P. M. (North-Holland, Amsterdam, 1970).

[10] S. P. Merkuriev, Theor. Math. Phys. **8**, 798 (1971);

[11] S. P. Merkuriev, Theor. Math. Phys. **32**, 680 (1977).

[12] S. P. Merkuriev, Lett. Math. Phys. **3**, 141 (1979).

[13] S. P. Merkuriev, Ann. Phys. **130**, 395 (1980).

[14] S. P. Merkuriev, C. Gignoux, A. Laverne, Ann. Phys. **99**, 30 (1976).

[15] A. Laverne, C. Gignoux, Institute des Sciences des Sciences Nucleaires, Internal Report 72-11.

[16] C. Gignoux, A. Laverne, Phys. Rev. Lett. **29**, 436 (1972).

[17] J. J. Benayoun, C. Gignoux, Nucl. Phys. **A190**, 419 (1972).

[18] A. Laverne, C. Gignoux, Nucl. Phys. **A203**, 597 (1973).

[19] L. D. Faddeev, S. P. Merkuriev, *Quantum Scattering Theory for Several Particle Systems* (Kluwer Academic Publishers, Dordrecht, The Netherland, 1993).

[20] S. P. Merkuriev, in *Proceedings of the Ninth European Conference on Few-Body Problems in Physics*, Eds. L. D. Faddeev , T. I. Kopaleishvili (World Scientific, 1984).

[21] H. P. Noyes, H. Fiedeldey, in *Three-particle scattering in Quantum Mechanics*, p. 195 Eds. J. Gillespie, J. Nuttall (Benjamin, New York, 1968).

[22] R. V. Reid, Annal. Phys. **50**, 411 (1968).

[23] E. P. Harper, Y. E. Kim, A. Tubis, Phys. Rev. Lett. **C6**, 126 (1972).

[24] E. Hadjimichael, A. D. Jackson, Nucl. Phys. **A180**, 217 (1972).

[25] S. N. Yang, A. D. Jackson, Phys. Lett. **36B**, 1 (1972).

[26] C. Gignoux, A. Laverne, S. P. Merkuriev, Phys. Rev. Lett. **33**, 1350 (1974).

[27] A. Brandenburg, Y. E. Kim, A. Tubis, Phys. Rev. **C12**, 1368 (1975).

[28] G. L. Payne, J. L. Friar, B. F. Gibson, I. R. Afnan, Phys. Rev. **C22**, 823 (1980).

[29] J. L. Friar, B. F. Gibson, G. L. Payne, Annu. Rev. Nucl. Sci. **34**, 403 (1984).

[30] C. R. Chen, G. L. Payne, J. L. Friar, B. F. Gibson, Phys. Rev. **C31**, 2266 (1985).

[31] C. R. Chen, G. L. Payne, J. L. Friar, B. F. Gibson, Phys. Rev. **C33**, 1740 (1986).

[32] V. V. Kostrykin, A. A. Kvitsinsky, S. P. Merkuriev, Few-Body Systems **6**, 97 (1989).

[33] N. W. Schellingerhout, L. P. Kok, G. D. Bosveld, Phys. Rev. **A40**, 5568 (1989).

[34] N. W. Schellingerhout, L. P. Kok, Nucl. Phys. **A508**, 299c (1990).

[35] L. P. Kok, N. W. Schellingerhout, Few-Body Systems **11**, 99 (1991).

[36] N. W. Schellingerhout, J. J. Schut, L. P. Kok, Phys. Rev. **C46**, 1192 (1992).

[37] N. W. Schellingerhout, *Factorizability in the Numerical Few-Body Problem* (PhD Thesis, University of Gröningen, The Netherlands (1995)).

[38] Ch. Elster, W. Schadow, A. Nogga, W. Glöckle, Few-Body Systems **27**, 83 (1998).

[39] W. Schadow, Ch. Elster, W. Glöckle, Few-Body Systems **28**, 15 (2000).

[40] H. Liu, Ch. Elster, W. Glöckle, LANL preprint: nucl-th/0204027.

[41] R. A. Malfliet, A. J. Tjon, Nucl. Phys. **A127**, 161 (1969).

[42] R. A. Malfliet, A. J. Tjon, Ann. of Phys. **61**, 425 (1970).

[43] I. E. Lagaris, V. R. Pandharipande, Nucl. Phys. **A359**, 331 (1981).

[44] I. E. Lagaris, V. R. Pandharipande, Nucl. Phys. **A359**, 349 (1981).

[45] C. H. Johnson, T. H. Spurling, Aust. J. Chem. **24**, 2205 (1971).

[46] A. A. Kvitsinsky, V. V. Kostrykin, S. P. Merkuriev, Sov. Phys. Dokl. **33**, 499 (1988).

[47] A. A. Kvitsinsky, V. V. Kostrykin, S. P. Merkuriev, Sov. J. Part. Nucl. **21**, 533 (1990).

[48] A. A. Kvitsinsky, Yu. A. Kuperin, S. P. Merkuriev, A. K. Motovilov, S. L. Yakovlev, Sov. J. Part. Nucl. **17**, 533 (1986).

[49] W. Glöckle, *The Quantum Mechanical Few-Body Problem* (Springer-Verlag Berlin Heidelberg (1983)).

[50] B. M. Axilrod, E. J. Teller, J. Chem. Phys. **11**, 299 (1943).

[51] Y. Muto, Proc. Phys. Math. Soc. Japan **17**, 629 (1943).

[52] V. Roudnev, S. Yakovlev, Comp. Phys. Commun. **126**, 162 (2000).

[53] V. A. Roudnev, S. L. Yakovlev, S. A. Sofianos, LANL preprint: physics/0204025 (2002).

[54] Y. Saad, *SPARSKIT: A basic tool kit for sparse matrix computations*. Technical report, Computer Science Department, University of Minnesota, Minneapolis, MN 55455, June 1994.

[55] R. E. Lynch, J. R. Rice, D. H. Thomas, Numer. Math. **6**, 185 (1964).

[56] Y. Saad, *Numerical Methods for Large Eigenvalue Problems* (Manchester University Press, Manchester (1992)).

[57] Y. Saad, Mathematics of Computation, **42**, 567 (1984).

[58] D. Ho, Numer. Math. **56**, 721 (1990).

[59] D. G. Papageorgiou, I. N. Demetropoulos, I. E. Lagaris, Comput. Phys. Commun. **109**, 227 (1998).

[60] F. V. Theos, I. E. Lagaris, D. G. Papageorgiou, Comput. Phys. Commun. **159**, 63 (2004).

[61] C. G. Broyden, J. Instit. Math. & Appl. **6**, 222 (1970). R. Fletcher, Comput. J. **13**, 317 (1970). D. Goldfarb, Math. Comput. **24**, 23 (1970). D. F. Shanno, Math. Comput. **24**, 641 (1970).

[62] R. Fletcher, C. Reeves, Comput. J. **7**, 149 (1964).

[63] E. Polak, G. Ribiere, Rev. Fr. Inf. & Rech. Oper. **16**, 35 (1969).

[64] J. J. Moré, *Lecture Notes in Mathematics*, **630**, 105 (1977).

[65] I. E. Lagaris, I. Likas, D. I. Fotiadis, Comput. Phys. Commun. **104**, 1 (1997).

[66] J. Carbonell, C. Gignoux, Few-Body Systems, Suppl. **7**, 270 (1994).

[67] A. A. Kvitsinsky, C.-Y. Hu, Few-Body Systems **12**, 7 (1992).

[68] C. E. Rolfs, W. S. Rodney, *Caudrons in the Cosmos*, (University of Chicago Press, Chicago, 1988).

[69] S. A. Rakityansky, S. A. Sofianos, L. Howell, M. Braun, V. B. Belyaev, Nucl. Phys. **A613**, 132 (1997).

[70] V. B. Belyaev, D. E. Monakhov, S. A. Rakityansky, N. V. Shevchenko, M. Braun, L. Howell, S. A. Sofianos, W. Sandhas, Nucl. Phys. **A631**, 720c (1998).

[71] D. E. Monakhov, V. B. Belyaev, S. A. Sofianos, S. A. Rakityansky, W. Sandhas, Nucl. Phys. **A635**, 257 (1998).

[72] N. V. Shevchenko, S. A. Rakityansky, S. A. Sofianos, V. B. Belyaev, J. Phys. **G25**, 95 (1999).

[73] E. W. Kolb, M. S. Turner, *The Early Universe*, (Addison-Wesley, New-York, 1990).

[74] M. L. Goldberg, K. M. Watson, *Collision Theory*, (John Wiley, New York, 1964).

[75] R. R. Roy, B. P. Nigam, *Nuclear Physics*, John Wiley, New York (1967).

[76] H. S. Picker, Phys. Rev. **C30**, 1751 (1984).

[77] W. A. Fowler, F. Hoyle, Astrophys. J. **9**, 201 (1964).

[78] V. R. Pandharipande, in *The Three-Body Force in the Three-Nucleon System*, (Lecture Notes in Physics, **260**, Springer-Verlag (1986)).

[79] J. Carlson, V. R. Pandharipande, R. B. Wiringa, Nucl. Phys. **A401**, 59 (1983).

[80] J. G. Zabolitzky, K. E. Schmidt, M. H. Kalos, Phys. Rev. **C25**, 1111 (1982).

[81] H. Horiuchi, Prog. Theor. Phys. **64**, 184 (1980).

[82] D. R. Thompson, I. Reichstein, W. McClure, Y. C. Tang, Phys. Rev. **185**, 1351 (1969).

[83] L. L. Howell, S. A. Sofianos, H. Fiedeldey, G. Pantis, Nucl. Phys. **A556**, 29 (1993).

[84] D. Baye, Phys. Rev. Lett. **58**, 2738 (1987).

[85] G. R. Satchler, L. W. Owen, A. J. Elwyn, G. L. Morgan, Nucl. Phys. **A112**, 1 (1969).

[86] S. Sack, L. C. Biedenharn, G. Breit, Phys. Rev. **93**, 321 (1954).

[87] N. W. Schellingerhout, L. P. Kok, S. A. Coon, R. M. Adam, Phys. Rev. **C48**, 2714 (1993).

[88] P. E. Shanley, Phys. Rev. **187**, 1328 (1969).

[89] W. Oehm, S. A. Sofianos, H. Fiedeldey, Phys. Rev. **42**, 2322 (1990).

[90] W. Oehm, S. A. Sofianos, H. Fiedeldey, M. Fabre de la Ripelle, Phys. Rev. **43**, 25 (1991).

[91] C. T. Christou, *Coincidence Reactions Based on a Three-Body Model of* ^{6}*Li*, PhD Thesis, The George Wasshington University, (1986).

[92] E. L. Berger, J. Qiu, Phys. Rev. **D40**, 3128 (1989).

[93] P. Chaumette, J. Deregal, G. Durand, J. Fabre, in *Future Polarization Physics at Fermilab*, Eds. E. Berger, J. G. Morfin, A. L. Read, A. Yokosawa, (Fermilab, Batavia, 1988).

[94] G. Chaumette, J. Deregal, G. Durand, J. Fabre, L. van Rossum, in *High Energy Spin Physics, Eighth International Symposium*, Ed. K. J. Heller, (AIP, New York, 1989).

[95] J. Ashman *et al.*, European Muon Collaboration, Phys. Lett. **B206**, 364 (1988).

[96] A. Masaike, S. Nurushev, A. Yokosawa, Fermilab proposal No. 809, (1990).

[97] V. I. Kukulin, V. M. Krasnopol'sky, V. T. Voronchev, P. B. Sazonov, Nucl. Phys. **A417**, 128 (1984).

[98] M. Born, R. Oppenheimer, Ann. Physik **84**, 457 (1927).

[99] F. Luo, G. C. McBane, G. Kim, C. F. Giese, W. R. Gentry, J. Chem. Phys. **98**, 3564 (1993).

[100] F. Luo, C. F. Giese, W. R. Gentry, J. Chem. Phys. **104**, 1151 (1996).

[101] W. Schöllkopf, J. P. Toennies, Science **266**, 1345 (1994).

[102] W. Schöllkopf, J. P. Toennies, J. Chem. Phys. **104**, 1155 (1996).

[103] A. K. Motovilov, S. A. Sofianos, E. A. Kolganova, Chem. Phys. Lett. **275**, 168 (1997).

[104] A. K. Motovilov, W. Sandhas, S. A. Sofianos, E. A. Kolganova, Euro. Phys. J. **D13**, 33 (2001).

[105] E. A. Kolganova, A. K. Motovilov, S. A. Sofianos, Phys. Rev. **A56**, R1686 (1997).

[106] V. R. Pandharipande, J. G. Zabolitzky, S. C. Pieper, R. B. Wiringa, U. Helmbrecht, Phys. Rev. Lett. **50**, 1676 (1983).

[107] B. D. Esry, C. D. Lin, C. H. Greene, Phys. Rev. **A54**, 394 (1996).

[108] E. Nielsen, D. V. Fedorov, J. S. Jensen, J. Phys. **B31**, 4085 (1998) & LANL preprint: physics/9806020.

[109] V. Efimov, Nucl. Phys. **A210**, 157 (1973).

[110] V. A. Roudnev, S. L. Yakovlev, LANL preprint: physics/9910030 (1999).

[111] W. L. McMillan, Phys. Rev. **138**, A442 (1965).

[112] R. A. Aziz, F. R. W. McCourt, C. C. K. Wong, Mol. Phys. **61**, 1487 (1987).

[113] R. A. Aziz, M. J. Slaman, J. Chem. Phys. **94**, 8047 (1991).

[114] K. T. Tang, J. P. Toennies, C. L. Yiu, Phys. Rev. Lett. **74**, 1546 (1995).

[115] S. P. Merkuriev, A. K. Motovilov, S. D. Yakovlev, Theor. Math. Phys. **94**, 306 (1993).

[116] S. P. Merkuriev, A. K. Motovilov, Lett. Math. Phys. **7**, 497 (1983).

[117] J. I. Steinfeld, S. M. Adler-Golden, J. W. Gallagher, J. Phys. Chem. Ref. Data **16**, 911 (1987).

[118] J. M. Flaud, C. Camy-Peyret, C. P. Rinsland, M. A. H. Smith, V. Malathy-Devi, *Atlas of Ozone Line Parameters from Microwave to Medium Infrared*, Academic Press, New York, (1990).

[119] J. M. Flaud, R. Bacis, Spectrochim. Acta **A54**, 3 (1998).

[120] Vl. G. Tyuterev, S. Tashkun, P. Jensen, A. Barbe, T. Cours, J. Mol. Spectrosc. **198**, 57 (1999).

[121] A. Barbe, C. Secroun, P. Jouve, J. Mol. Spectrosc. **49**, 171 (1974).

[122] J. N. Murrell, S. Carter, S. C. Farantos, P. Huxley, A. J. C. Varandas, *Molecular Potential Energy Functions*, John Wiley & Sons, (1984).

[123] A. J. C. Varandas, J. N. Murrell, Chem. Phys. Lett. **1**, 88 (1982).

[124] R. Siebert, R. Schinke, M. Bittererova, Phys. Chem. Chem. Phys. **3**, 1795 (2001).

[125] W. J. Meath, R. A. Aziz, Mol. Phys. **52**, 225 (1984).

[126] G. A. Evangelakis, J. P. Rikos, I. E. Lagaris, I. N. Demetropoulos, Comput. Phys. Commun. **46**, 402 (1977).

[127] D. G. Papageorgiou, C. S. Chassapis, I. E. Lagaris, Comput. Phys. Commun. **52**, 241 (1989).

[128] R.O. Jones, Phys. Rev. Lett. **52**, 2002 (1984).

Appendix C

Dedication

I dedicate this thesis to the following persons who profoundly influenced and shaped my life. My

- grandmother Mankurube Mahlaela (10-April-1900 – 04-November-1997).
- father Makgale Johannes Lekala (circa. 1921 – 02-September-1976).
- mother Madire Lekala (28-July-1921 –).

For all their endeavours in trying to make me a better person, I pass the following quote:

> "It takes a long time to acquire the art, but life is short, the crisis rapid, experimentation dangerous, the cure uncertain"

From *Hippocrates, The first Aphorisms* [Paraphrased]